ELSEVIER

Journal of Structural Geology 30 (2008) 410–430

JOURNAL OF STRUCTURAL GEOLOGY

www.elsevier.com/locate/jsg

The initiation and evolution of the transpressional Straight River shear zone, central Fiordland, New Zealand

Daniel S. King [a,*], Keith A. Klepeis [a], Arthur G. Goldstein [b], George E. Gehrels [c], Geoffrey L. Clarke [d]

[a] *Department of Geology, University of Vermont, Burlington, VT 05405-0122, USA*
[b] *Department of Geology, Colgate University, Hamilton, NY 13346, USA*
[c] *Department of Geosciences, University of Arizona, 1040 E 4th Street, Tucson, AZ 85721, USA*
[d] *School of Geosciences, F09, University of Sydney, NSW 2006, Australia*

Received 12 July 2007; received in revised form 5 December 2007; accepted 5 December 2007
Available online 23 December 2007

Abstract

Structural data and U/Pb geochronology on zircon from central Fiordland, New Zealand show the role of pre-existing structural heterogeneities in the kinematic evolution of a newly discovered zone of transpression. The Straight River shear zone consists of steep zones of high strain that are superimposed onto older fabrics across a 10×80 km region. The older foliation formed during two periods of tectonism: contraction and magmatism of mostly Carboniferous ($\sim$312–306 Ma) age and Early Cretaceous batholith emplacement ending by 113.4 ± 1.7 Ma followed by extension that ceased by 88.4 ± 1.2 Ma. The primary mechanism for the formation of steep shear zone foliations was the folding of these older fabrics. Conjugate crenulation cleavages associated with the folding record shortening at high angles to the shear zone boundaries. Fold axial surfaces and axial planar cleavages strike parallel to the shear zone with increasing strain as they progressively steepened to subvertical. In most areas, shear sense flips from oblique-sinistral (east-side-down component) to oblique-dextral (west-side-down) across zones of intermediate and high strain. High strain zones display subvertical mineral lineations, steep strike-slip faults and shear sense indicators that record strike-slip motion across the steep lineations. These patterns reflect triclinic transpression characterized by narrow zones of mostly strike-slip deformation and wide zones of mostly contraction. Zones of high strain align with offshore traces of late Tertiary strike-slip faults, suggesting that a previously undocumented component of late Tertiary shortening and strike-slip motion is accommodated within Fiordland.

Keywords: Transpression; Shear zone; Strain partitioning; U/Pb geochronology

1. Introduction

Transpression refers to deformation that accommodates simultaneous flattening and shearing and is commonly observed at oblique plate margins (Harland, 1971). One of the first three-dimensional kinematic models for transpression was introduced by Sanderson and Marchini (1984), and many subsequent studies have modified this model and its boundary conditions to explore the complex three-dimensional strain patterns that are possible with transpression (e.g. Fossen and Tikoff, 1993; Jones et al., 1997, 2004; Robin and Cruden, 1994; Jiang et al., 2001). These and most other mathematical models generally assume homogeneous deformation within the block being deformed. However, zones of continental deformation typically are characterized by heterogeneous strain patterns, including displacements that are distributed non-uniformly across large areas. Kinematic partitioning, where components of strike-slip and dip-slip motion occur in different places and on separate structures, is especially common in zones of oblique convergence and has been documented in many orogens and continental transforms

* Corresponding author. Present address: University of Minnesota, Department of Geology and Geophysics, 310 Pillsbury Drive SE, Minneapolis, MN 55455, USA. Tel.: +1 612 626 0572; fax: +1 612 625 3819.
E-mail address: king0314@umn.edu (D.S. King).

0191-8141/$ - see front matter © 2007 Elsevier Ltd. All rights reserved.
doi:10.1016/j.jsg.2007.12.004

(e.g. Mount and Suppe, 1987; McCaffrey, 1992; Goodwin and Williams, 1996; Butler et al., 1998; Norris and Cooper, 2001; Bhattacharyya and Hudleston, 2001; Claypool et al., 2002; Fuis et al., 2003; Holdsworth et al., 2002; Czeck and Hudleston, 2003; Barnes et al., 2005; Sutherland et al., 2006). Previous work has shown that the controls on kinematic partitioning, and the evolution of obliquely convergent zones in general, can include far-field plate boundary conditions (e.g. Teyssier et al., 1995; Jiang et al., 2001; Tikoff et al., 2002), rheological contrasts in the crust (e.g. Coke et al., 2003; Marcotte et al., 2005), and the presence of mechanical heterogeneities such as old faults and shear zones (e.g. Mount and Suppe, 1987; Vauchez et al., 1998; Tavarnelli et al., 2004). Determining which of these factors exerts the dominant control on zones of oblique convergence, and at which scale, is important for understanding how orogenic belts develop in different settings.

Variations in the style or degree of strike-slip partitioning commonly occur along the strike of major fault zones such as the Alpine fault, which has accommodated at least 460 km of dextral movement since 20–25 Ma (Wellman, 1953; Sutherland, 1999). Oblique-slip on the central section of the Alpine fault (Fig. 1a) provides an example of a system characterized by a low degree of strike-slip partitioning (Norris et al., 1990; Berryman et al., 1992; Teyssier et al., 1995; Little, 1996; Norris and Cooper, 1995, 2001). Along this segment, the Alpine fault strikes to the northeast (55°), dips moderately to the southeast and displays a slip direction that plunges ~22°. The remaining motion is distributed on thrust and oblique-slip faults in a >100 km-wide zone located mostly east of the Alpine fault. In contrast, the Fiordland (southernmost) segment of the Alpine fault is nearly vertical and accommodates almost pure strike-slip motion (Barnes et al., 2001, 2005). Folds and reverse faults west and east of the Alpine fault accommodate contraction, indicating that this part of the Alpine fault system is strike-slip partitioned (Norris et al., 1990; Markley and Norris, 1999; Claypool et al., 2002; Barnes et al., 2001, 2005). However, the amount of shortening accommodated by these structures has been difficult to quantify (Norris and Cooper, 2001).

In this paper, we examine how lithologic heterogeneity and pre-existing mechanical anisotropies controlled the initiation and evolution of a large transpressional shear zone of apparent late Tertiary age in Fiordland, New Zealand. The Straight River shear zone (Fig. 1), which is located southeast of the southernmost segment of the Alpine fault, was first identified by Oliver and Coggon (1979) as the Straight River [thrust] fault and is interpreted here as a transpressional structure on the basis of new data. This reinterpretation shows the existence of a previously undocumented component of contraction

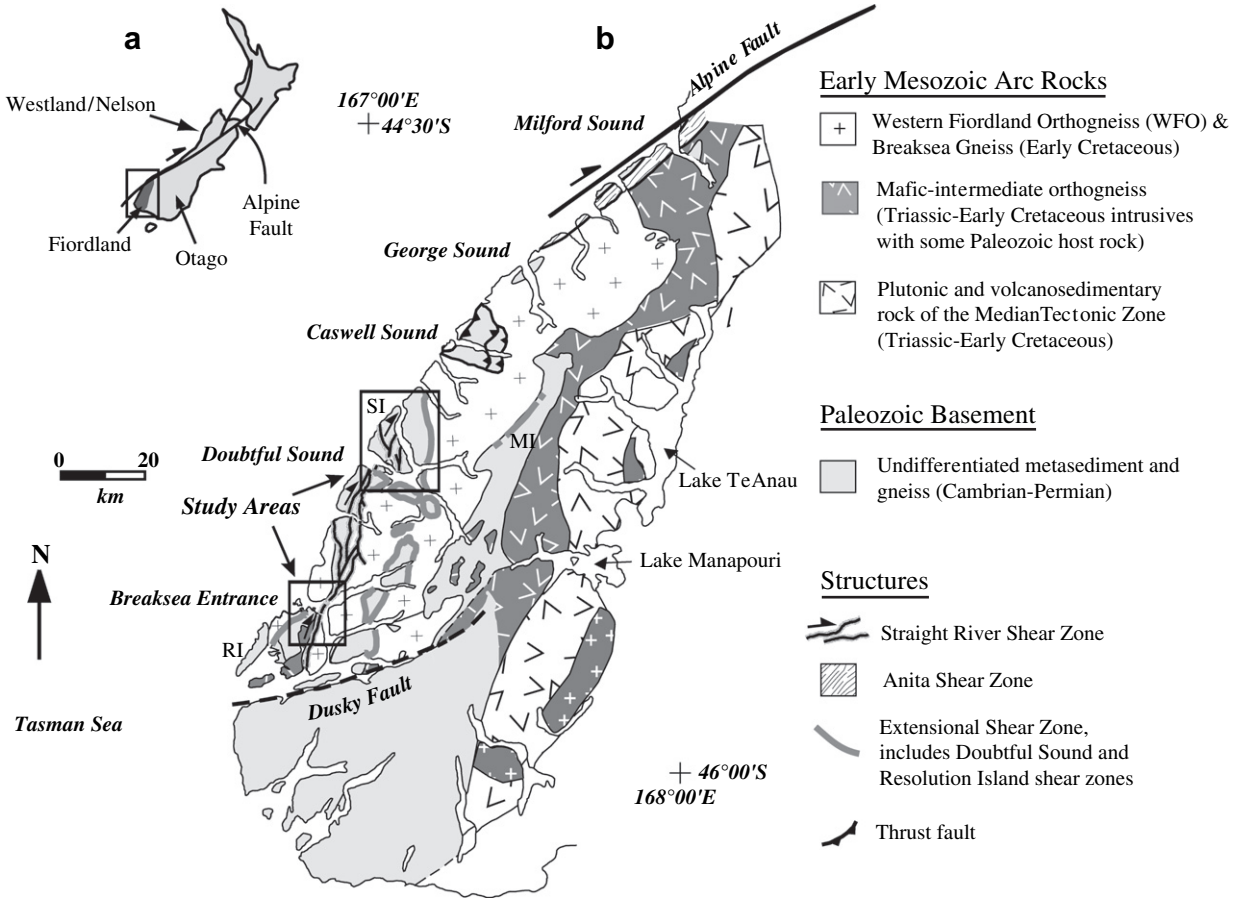

Fig. 1. (a) Sketch map showing location of Fiordland and Westland–Nelson regions. (b) Geological map of Fiordland (after Bradshaw, 1990). SI – Secretary Island; RI – Resolution Island; MI – Mt. Irene.

accommodated in Fiordland in the early stages of the formation of the Alpine fault. An especially interesting aspect of our study is the analysis of outcrops that record the progressive development of a heterogeneous array of structures that record different combinations of contraction and strike-slip deformation. In particular, a progressive tightening of asymmetric folds and the rotation of fold axial planes during shortening at high angles to the shear zone boundaries controlled the development of steep foliation planes, down-dip and oblique mineral lineations, and other structures commonly viewed as diagnostic of transpression. This field-based model illustrates a mechanism for the formation of vertical structures in rocks with a pre-existing foliation. Our results provide information on the types and scales of anisotropies that influence the formation and evolution of ductile structures in a newly discovered zone of transpression that affects at least 800 km^2 of crust. This style of transpressional deformation is characterized by smaller-scale partitioning of deformation than the documented partitioning between the Alpine fault system and offshore fold-thrust belts.

2. Regional tectonic history of Fiordland

Central Fiordland (Fig. 1) records a history of orogenesis that occurred between ~481 and ~334 Ma (Oliver, 1980; Gibson et al., 1988; Ireland and Gibson, 1998). Crustal thickening is indicated by kyanite-bearing assemblages (recording pressures of 7–9 kb) that overprint higher-temperature and lower pressure ($P = 3–5$ kb) sillimanite-bearing assemblages in Paleozoic gneiss (Gibson, 1990). The relatively high-T, low-P event occurred at ~360 Ma (Ireland and Gibson, 1998; Gibson and Ireland, 1999), the high-P phase of metamorphism (7–9 kb) occurred at ~330 Ma (Ireland and Gibson, 1998).

Superimposed on these Paleozoic metamorphic rocks is a record of Early Cretaceous arc magmatism, upper amphibolite to granulite facies metamorphism, and contraction (Oliver, 1977; Bradshaw, 1989; Gibson and Ireland, 1995; Mortimer et al., 1999; Daczko et al., 2001; Klepeis et al., 2004). A major batholith was emplaced into the middle and the lower crust from ~126 to ~113 Ma and subsequently deformed to form the Western Fiordland Orthogneiss (Mattinson et al., 1986; McCulloch et al., 1987; Gibson et al., 1988; Gibson and Ireland, 1995; Tulloch and Kimbrough, 2003; Hollis et al., 2004). Similar intrusions comprise the protolith of the Breaksea Gneiss (Fig. 1). Mineral assemblages indicate that metamorphism at pressures of at least 12–14 kb occurred in both batholiths (Oliver, 1977; Bradshaw, 1989; Clarke et al., 2000; Daczko et al., 2001).

By ~114 Ma western New Zealand was dominated by extension and crustal thinning (Tulloch and Kimbrough, 1989; Spell et al., 2000). The extensional Doubtful Sound and Resolution Island shear zones formed after ~111 Ma (Oliver and Coggon, 1979; Oliver, 1980; Gibson and Ireland, 1995; Ireland and Gibson, 1998; Klepeis et al., 2007).

Exhumation of rocks representative of Early Cretaceous middle and lower crust occurred mostly during the Mid-Late Cretaceous as a result of extension (Flowers et al., 2005; Klepeis et al., 2007). Metamorphic core complexes formed during this period (Tulloch and Kimbrough, 1989; Allibone and Tulloch, 1997; Spell et al., 2000; Turnbull and Allibone, 2003; Kula et al., 2005; Klepeis et al., 2007). The extension culminated in the rifting of New Zealand from Australia and Antarctica and the initiation of seafloor spreading in the Tasman Sea by ~84 Ma (Gaina et al., 1998; Kula et al., 2005). Exhumation following Late Cretaceous extension was slow until the onset of late Cenozoic transpression (House et al., 2002). In northern Fiordland, this exhumation history is recorded by superposed structures in the Anita shear zone (Fig. 1; Hill, 1995; Klepeis et al., 1999).

By ~52 Ma, sea floor spreading in the Tasman Sea had ended (Gaina et al., 1998). The Pacific–Australia plate boundary developed as a spreading center south of New Zealand by 47–45 Ma (Sutherland et al., 2000). From 30 to 11 Ma, spreading became progressively more oblique and the boundary evolved into a transform (Lamarche et al., 1997). Subduction beneath Fiordland and formation of the Alpine fault began as early as 25–20 Ma (Lebrun et al., 2003; Lamarche and Lebrun, 2000).

3. Structural and kinematic analysis

In this section we describe structures from the Doubtful Sound region (Fig. 1) where we studied the SRSZ and older structures in detail. We compare these elements to those exposed at Breaksea Entrance to evaluate their along-strike variability. The analysis of Paleozoic and Mesozoic structures allows us to determine how older structures influenced the evolution of subsequent phases of deformation. The Doubtful Sound region is characterized by three structural domains (Fig. 2). Domain I preserves structures associated with Paleozoic deformation, granitic magmatism, and metamorphism. Domain II preserves structures and metamorphic mineral assemblages associated with Early Cretaceous magmatism and mid-Cretaceous extension. Domain III preserves structures associated with the formation of the younger SRSZ.

3.1. Paleozoic rock units and structures (domain I)

Domain I (Fig. 2a) contains schist, paragneiss, and orthogneiss of the Deep Cove Gneiss. At the west end of Doubtful Sound, and on Secretary Island (Fig. 3), the thickest unit is a micaceous meta-arenite. Garnet amphibolite, calc-silicate, and marble layers are also present. In most areas of domain I, bedding (S_0) is overprinted by deformation and upper amphibolite facies metamorphism. However, near the southeast headland of Secretary Island we observed relict cross-bedding (Fig. 4a) and graded beds in tightly folded (F_1) meta-arenite layers (Fig. 4b). The folds are overturned and recumbent, and display an axial planar foliation (S_1) defined by biotite in schist and hornblende + plagioclase aggregates in garnet amphibolite units. Aligned biotite and hornblende define mineral elongation lineations (L_1) in these units, respectively (Fig. 4b, inset).

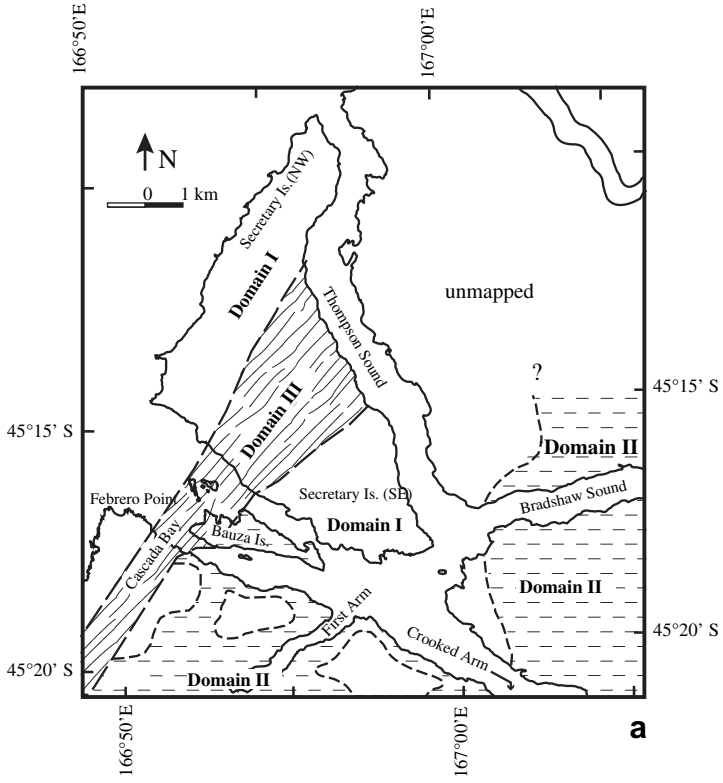

b

		Domain I			Domain II			Domain III			
		Febrero Pt.	Secretary Is. NW	Secretary Is. SE	First Arm	Bradshaw Sound	Crooked Arm	Cascada Bay	Western Bauza Is.	Thompson Sound	Description/ Assemblage
Structures Within Metasediments (Paleozoic)	S_0		×	×							graded bedding
	S_1,L_1	×	×	×				×	×	×	biotite
	Granitoid/Amphibolite Sheets	×	×	×							
	F_2 Recumbent Folds	×	×								
Intrusives and Extension (Mesozoic)	S_{WFO}				×	×	×				amph +/- cpx +/- biot
	GRZ veins				×		×				garnet, cpx
	S_{GRZ}						×				
	S_{DS}, L_{DS}, F_{DS}				×	×	×	×	×		biot, amph, qtz
	Secretery Is. Syncline		×	×							
SRSZ Structures (Mesozoic/ Cenozoic)	F_{SR}							×	×	×	
	S_{cr1},S_{cr2}									×	biotite
	S_{SR},L_{SR}				×		×	×	×	×	biot, musc,calcite, amph
Brittle Faulting (Tertiary)	Faults	×	×	×	×					×	epidote fault surfaces
	Fractures	×	×	×	×	×	×	×	×	×	

Fig. 2. (a) Map showing structural domains surrounding Secretary Island. (b) Fabric elements associated with each domain. See text for definitions.

At least two generations of granitic dikes intrude the Deep Cove gneiss. The first cuts the L_1–S_1 fabric and is folded into tight inclined-recumbent folds (F_2) (Fig. 4c). The folds display an axial planar foliation (S_2). The second generation of dikes cuts the first and forms thick (several meters), weakly deformed tabular bodies (Fig. 4d). One of the largest of these latter bodies is the Deas Cove Granite (Fig. 3), which yielded an Rb/Sr whole-rock age of 372 ± 12 Ma (Oliver, 1980). These

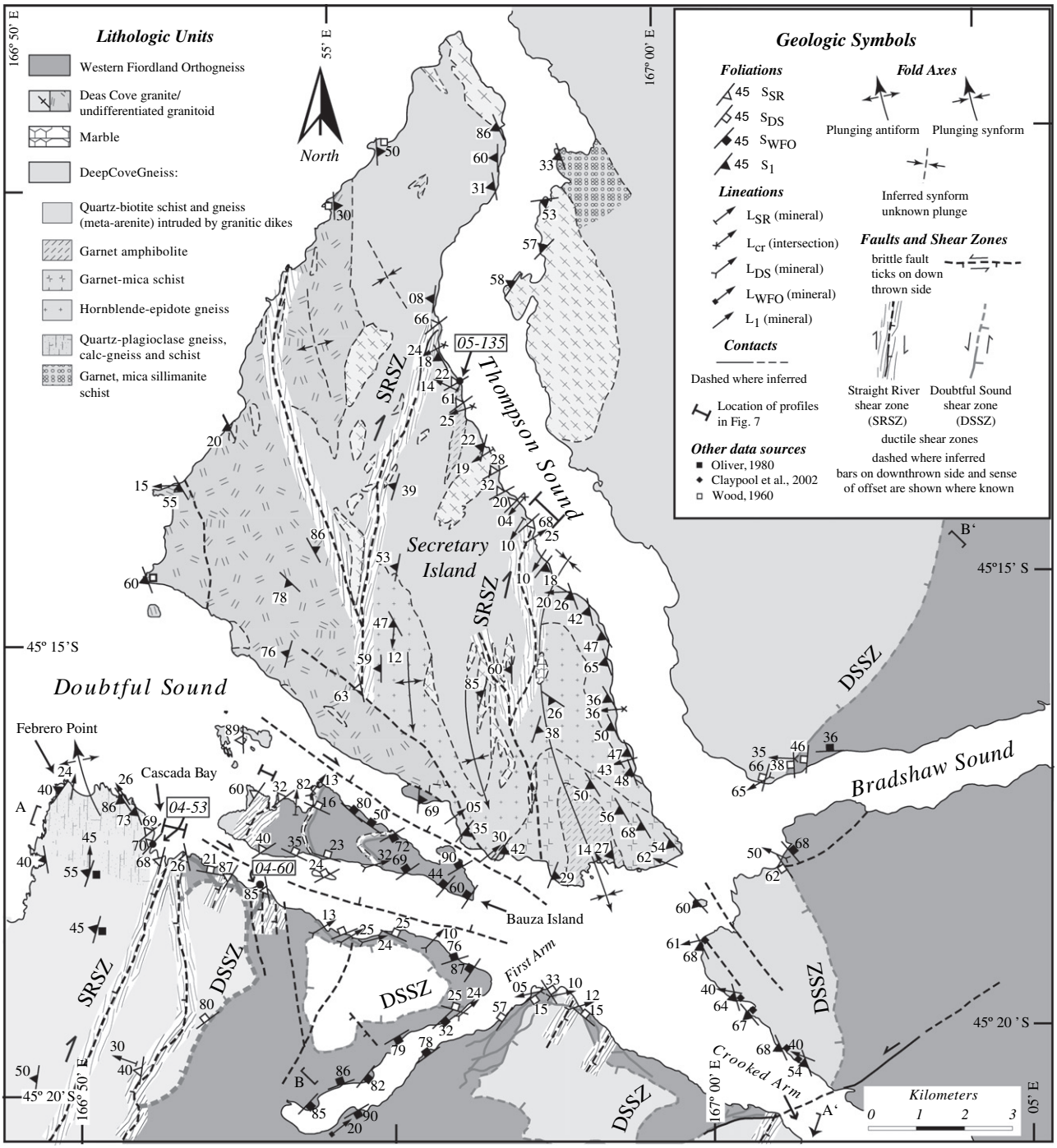

Fig. 3. Geological map showing major structures and lithologic units in Doubtful, Thompson, and Bradshaw Sounds. Maps of the interior of Secretary Island were completed by I. Turnbull and others at the Institute for Geological and Nuclear Sciences in Dunedin. Cross-sections A–A′ and B–B′ are shown in Fig. 5. Samples locations are indicated (Wood, 1960).

observations show that the regional fabric in domain I formed as mid-Paleozoic granitoids intruded a thick sequence of volcanic and sedimentary rocks.

3.2. Mesozoic intrusive rock and extensional structures (domain II)

The Western Fiordland Orthogneiss contains several distinctive mineral assemblages, including garnet- and clinopyroxene-bearing veins that record garnet granulite facies metamorphism at depths >45 km (Oliver, 1977, 1980; Gibson and Ireland, 1995; Hollis et al., 2004). These garnet granulite assemblages are recrystallized within the retrogressive, upper amphibolite facies Doubtful Sound shear zone (Figs. 3 and 5e, f). Klepeis et al. (2007) showed that these superposed assemblages record a progressive change in temperature, pressure, and fluid conditions in the lower crust and create a regional gneissic layering that characterizes domain II (Figs. 2 and 5f–h).

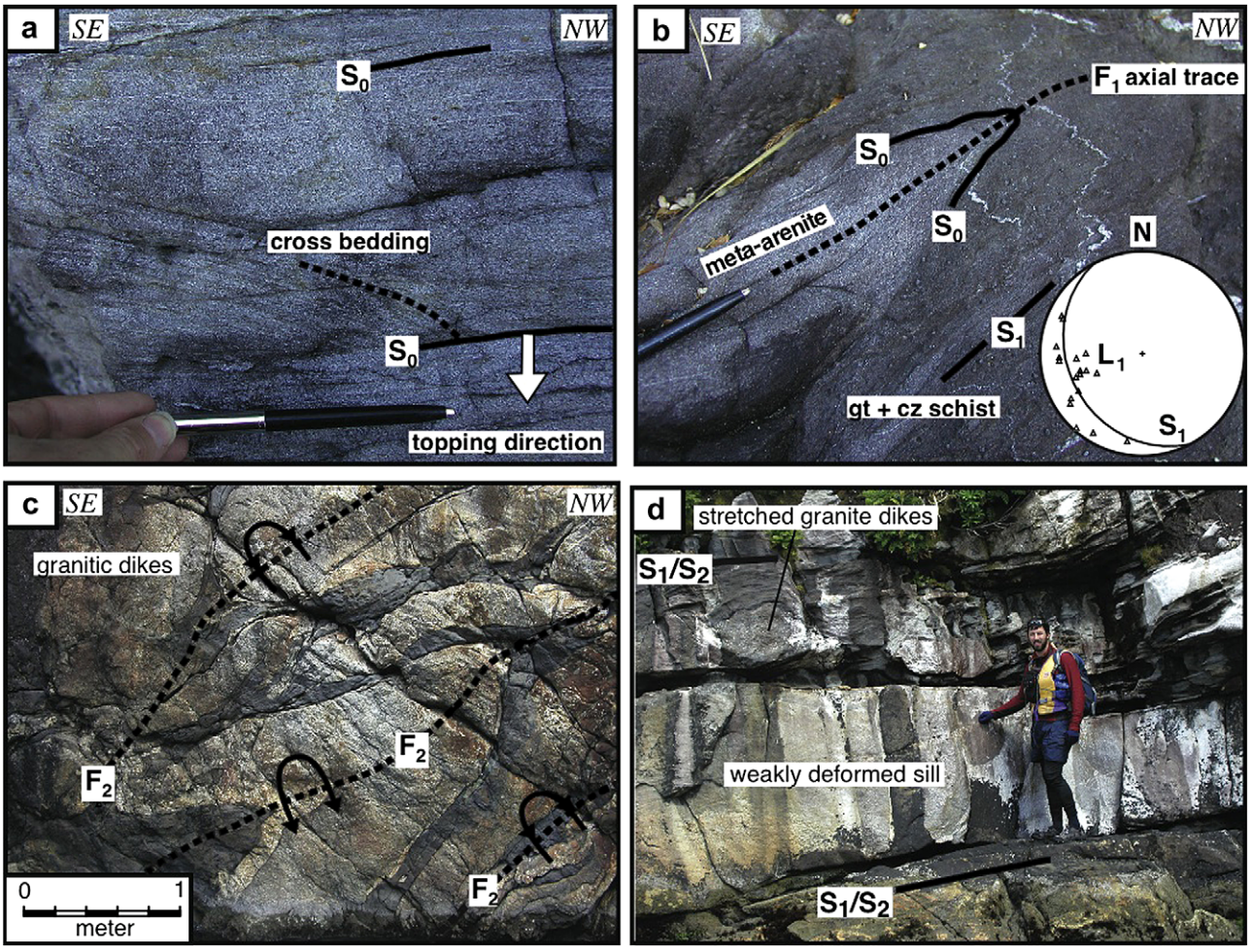

Fig. 4. Structures exposed along Thompson Sound that predate the SRSZ. (a) Overturned cross-bedding (S_0) in meta-arenite. (b) Folded (F_1) meta-arenite layer in garnet (gt) + clinozoisite (cz) schist with an axial planar cleavage (S_1). Inset shows L_1 mineral lineations and the average S_1 cleavage orientation plotted on an equal area lower hemisphere projection. (c) First generation of granitic dikes are folded into tight F_2 folds. (d) Second generation of dikes are weakly deformed and of mostly Carboniferous age (Fig. 11g).

The Doubtful Sound shear zone is composed of folded, attenuated and locally mylonitic layers of marble, calc-silicate gneiss and orthogneiss. The orientation of high strain zones is variable. Along Doubtful Sound they dip 20–30° to the east–northeast (Fig. 5b, f, h). Top-down-to-the-northeast and -southwest sense-of-shear indicators are consistent with interpretations of the shear zone as a ductile normal fault (Gibson et al., 1988; Oliver, 1990; Klepeis et al., 2007).

On Resolution Island, (within the southernmost study site, Fig. 6) the Cretaceous Breaksea Gneiss is composed primarily of granulite and, locally, eclogite facies metagabbro and metadiorite that is similar to, but more mafic than, the metagabbro of the Western Fiordland Orthogneiss. Unretrogressed parts of this unit have yielded peak metamorphic pressures ranging from 11 kbar to at least 15–16 kbar (Allibone et al., 2005; Milan et al., 2005; M. De Paoli, personal communication, 2007), the highest pressures recorded in Fiordland. Like the Doubtful Sound shear zone, the Resolution Island shear zone (Fig. 6) is defined by heterogeneous upper amphibolite facies high strain zones that form a regional flat to moderately dipping foliation (Klepeis et al., 2007).

3.3. The Straight River shear zone (domain III)

The Straight River shear zone (SRSZ) is a new name given to an array of steep high strain zones between Thompson Sound and Resolution Island (Figs. 3 and 7a). Oliver (1980) suggested that the part of this structure south of Doubtful Sound (the Straight River fault) was a major thrust fault that parallels the Doubtful Sound shear zone. We present new data that show the regional extent of the shear zone, its kinematic evolution, and its crosscutting relationship with the Doubtful Sound shear zone (Fig. 5). We completed four detailed transects across the shear zone and developed criteria for defining low, medium and high strain zones that qualitatively define the gradational boundaries of the SRSZ (Figs. 7 and 9).

3.3.1. Thompson Sound transect

Along Thompson Sound, the SRSZ lies entirely within Paleozoic meta-arenite that is intruded by minor granitoids (Fig. 7b). This transect is important because the relative uniformity of the meta-arenite lithology (Fig. 7b) allowed us to

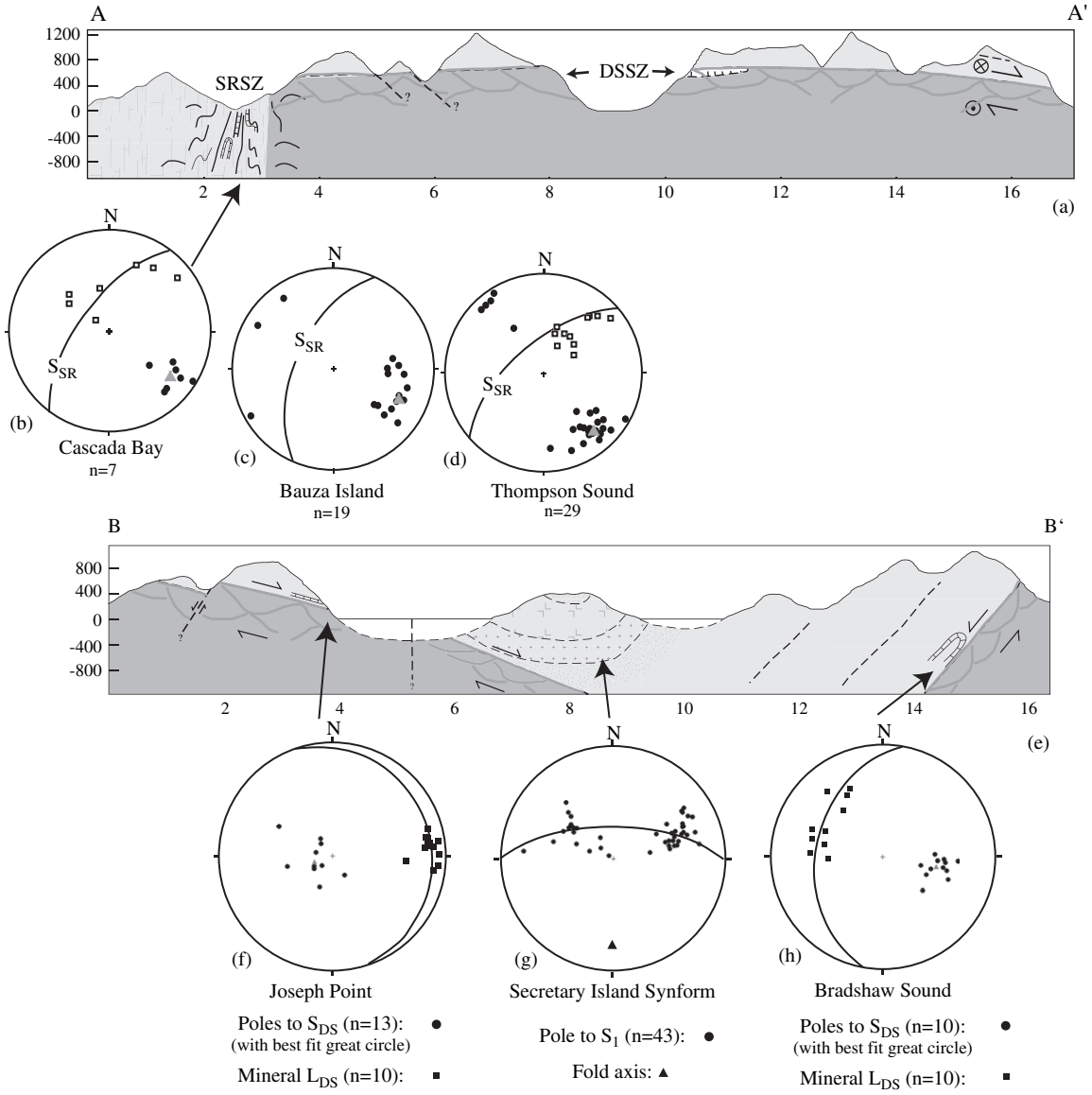

Fig. 5. (a) Cross-section A–A′ (location in Fig. 3) showing the S_{SR} cutting the Doubtful Sound shear zone. (b), (c), (d) Poles to S_{SR} foliation (circles) in the SRSZ with best fit great circle at the locations of three detailed sketches shown in Fig. 7. Plots are lower hemisphere, equal area projections. White squares are quartz–biotite mineral lineations (L_{SR}). (e) Section B–B′ showing antithetic/synthetic pair of extensional shear zones at Doubtful and Bradshaw sounds. (f) Poles to S_{DS} foliation (circles) with best fit great circle and L_{DS} (squares). (g) π-diagram of poles to S_1 defining a F_2 fold axis. (h) Poles to S_{DS} foliation (circles) with best fit great circle and L_{DS} (squares) at Bradshaw Sound.

rule out the effects of different lithologies as a cause of structural variability. At northern and southern boundaries of the shear zone (Fig. 3), pre-existing S_1 foliation is cut by a steep shear zone foliation that dips steeply away from the center of the shear zone (S_{SR}). The outer ~1 km of domain III at Thompson Sound (Fig. 2a) is characterized by zones up to several meters wide composed of steep shear zone foliation planes. Pre-existing S_1 foliation planes are deflected, folded and transposed into the S_{SR} shear zone foliation in these zones. Between these discrete zones the fabric is dominated by more gently dipping pre-existing S_1 foliation planes. This pattern of deformation allowed us to determine the orientation of the boundaries of high strain zones.

In the center of domain III, all Paleozoic structures are overprinted by SRSZ structures. Fig. 9a shows a monocline exposed in a low strain zone northwest of the center high strain zone along Thompson Sound. Compositional layering is folded into monoclines and small-scale asymmetric folds that display northwest dipping axial planes. The opposite asymmetry (i.e. southeast-dipping axial planes of monoclines) occurs on the southeast side of the SRSZ on Bauza Island (Fig. 7c). The orientations of folded pre-existing S_1 foliation planes (Fig. 9b) from within a ~50 m section of folds display a southwest-plunging calculated fold axis that coincides with measured fold hinges. The axial planes dip to the northwest. We interpret these monoclines to characterize a low strain zone that records an early stage in the evolution of shear zone folds.

Crenulation cleavage occurs throughout the transect (Figs. 8c and 9c). The cleavage is best developed in the micaceous

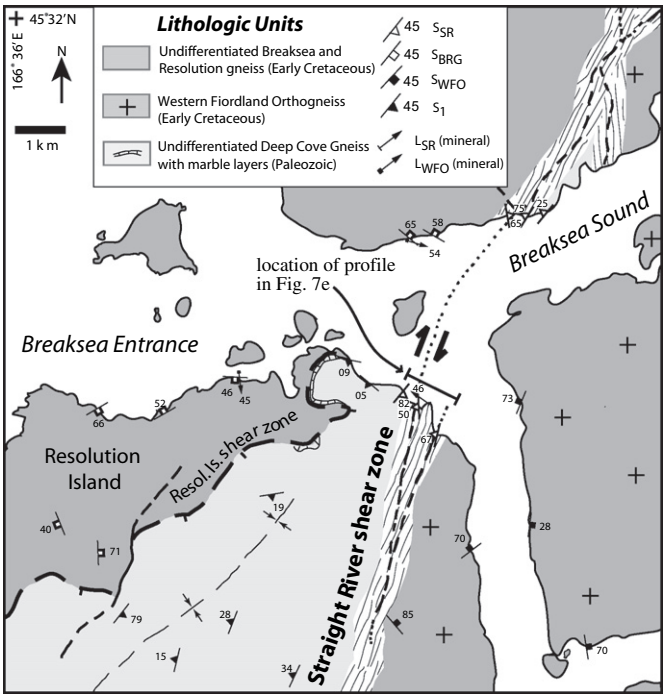

Fig. 6. Simplified geological map of Breaksea Entrance showing the southern strand of the SRSZ. Geologic symbols are the same as in Fig. 3 except foliation with white boxes, which represents part of the extensional Resolution Island shear zone. Map of Resolution Island combines data collected along the coastlines by the authors and data from the interior of the island from Turnbull et al. (2005), Allibone et al. (2005) and Milan et al. (2005).

meta-arenite layers where dominant crenulation cleavage planes (S_{cr1}) strike ~110° and dip ~65° to the southwest. The subordinate crenulation cleavage planes (S_{cr2}) strike ~48° and dip ~80° to the northwest (Fig. 8e). The two sets always occur together and form angles of 112° and 68° with one another. These zones, with two well-developed sets of crenulation cleavage and relatively tight, inclined folds, define our intermediate strain zones (Fig. 9c, f).

Within high strain zones at the center of the zone of deformation, S_{cr2} is more pronounced than it is elsewhere and S_{cr1} is less defined if present at all. The center of the SRSZ is defined by zones where pre-existing foliation is completely transposed into a steep shear zone foliation that is parallel to the S_{cr2} plane. Shear zone fold hinges are nearly vertical and folds are significantly tighter than the intermediate strain zones on either side of the high strain zone. Between these high strain zones of steeply dipping shear zone foliation and isoclinal folds are intermediate strain zones where both crenulation cleavage planes are visible. In the transition zones near shear zone boundaries, both crenulation cleavage orientations coexist and pre-existing S_1 is folded into recumbent and monoclinal shear zone folds with axial planes that dip away from the center of the zone of deformation.

3.3.2. Cascada Bay transect

Located 2 km inland from the Tasman Sea (Fig. 3), Cascada Bay (Fig. 3) displays evidence for the localization of strain within a marble-rich sequence and a strain gradient defined by variations in fold tightness and a decrease in the degree of transposition toward the center of the shear zone. East of the bay, the Doubtful Sound shear zone foliation (S_{DS}) within the Western Fiordland Orthogneiss is folded into broad, open SRSZ folds (F_{SR}) (Fig. 7d). Close to the contact between the orthogneiss and the marble-rich sequence (Fig. 7d), folds are tight and the steep shear zones are common, defining a qualitative increase in strain to the west toward Cascada Bay at high angles to the SRSZ boundaries. Structures exposed at Cascada Bay indicate that strain is focused into a ~250 m-wide zone within the marble-rich sequence. In low and intermediate strain zones, SRSZ fold axial planes dip to the SW and NE in recumbent and inclined monoclinal folds (Fig. 9d). In zones that record higher strain closer to the center of the shear zone, SRSZ fold axial planes are nearly vertical and are subparallel to the SRSZ foliation (Fig. 7d). Fold hinges plunge ~80° to the north–northwest. The contact between the marble-rich sequence and the calc-silicate gneiss to the west is sheared and displays the subvertical SRSZ foliation. Farther west, the pre-existing S_1 foliation is folded into SRSZ folds and locally transposed into the shear zone foliation. These folds gradually open up to the west defining a gradational boundary between domains III and I (Fig. 2a).

3.3.3. Straight River shear zone structures in the Western Fiordland Orthogneiss

Structures associated with the SRSZ in the Western Fiordland Orthogneiss occur up to ~6 km east of the high strain zone at Cascada Bay (Fig. 10). The Doubtful Sound shear zone foliation (S_{DS}) is folded and transposed into the steep SRSZ foliation (S_{SR}) in 10 m-wide high strain zones (e.g. Fig. 9e) that are spaced a few hundred meters to several

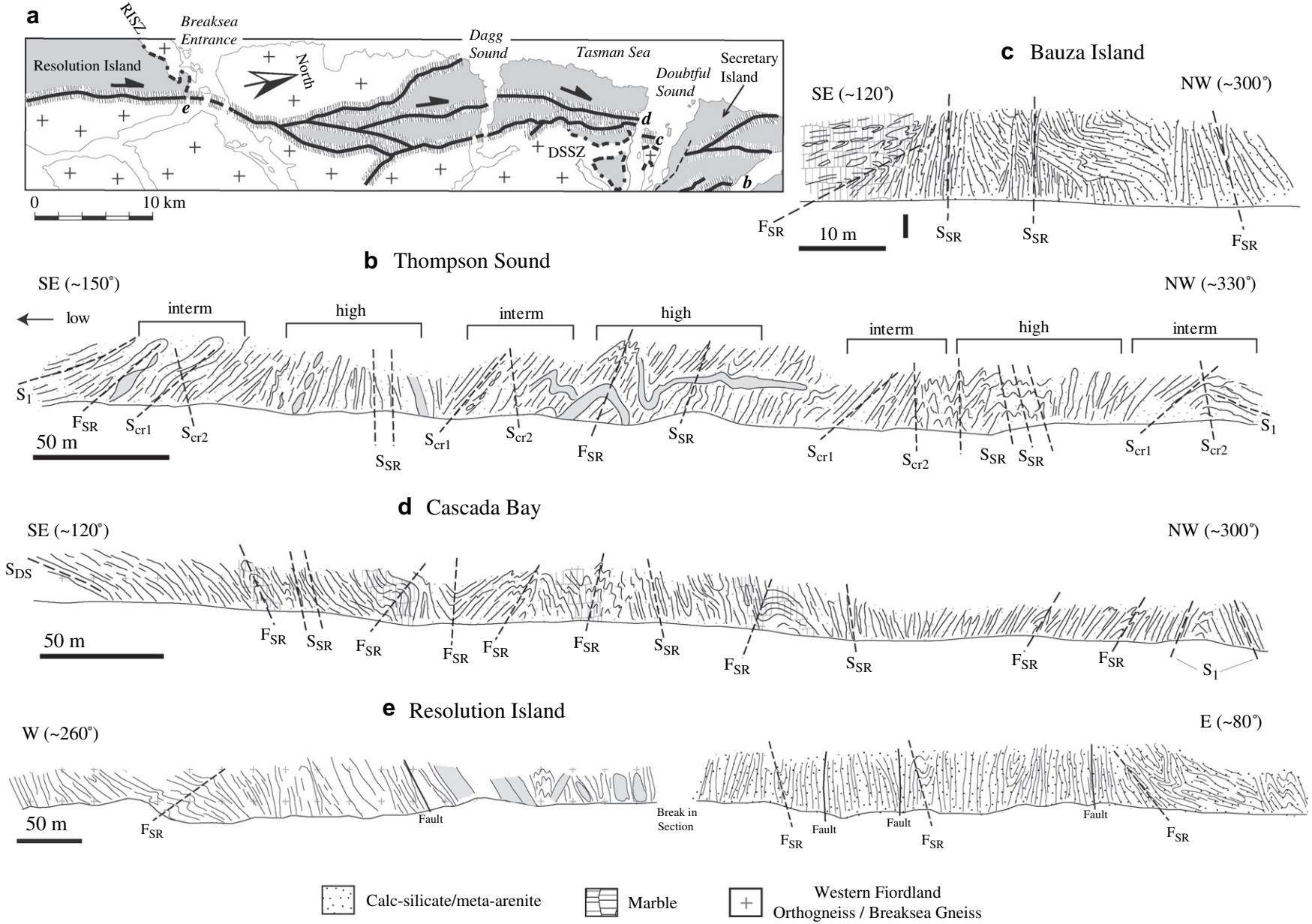

Fig. 7. (a) Simplified map showing the known extent of the SRSZ and the locations of four profiles at (b) Thompson Sound (c) Bauza Island (d) Cascada Bay, and (e) Resolution Island. Map patterns are Paleozoic gneiss (shaded grey) and Early Cretaceous Western Fiordland Orthogneiss and Breaksea Gneiss (crosses). Profiles show orientations of fabric elements (S_1, S_{cr1}, S_{cr2}, F_{SR}, and S_{SR}) defined in text. Shaded areas in (b) are granitic dikes. Other than the dikes, this transect is composed of a relatively uniform meta-arenite lithology. The other three transects contain multiple lithologies.

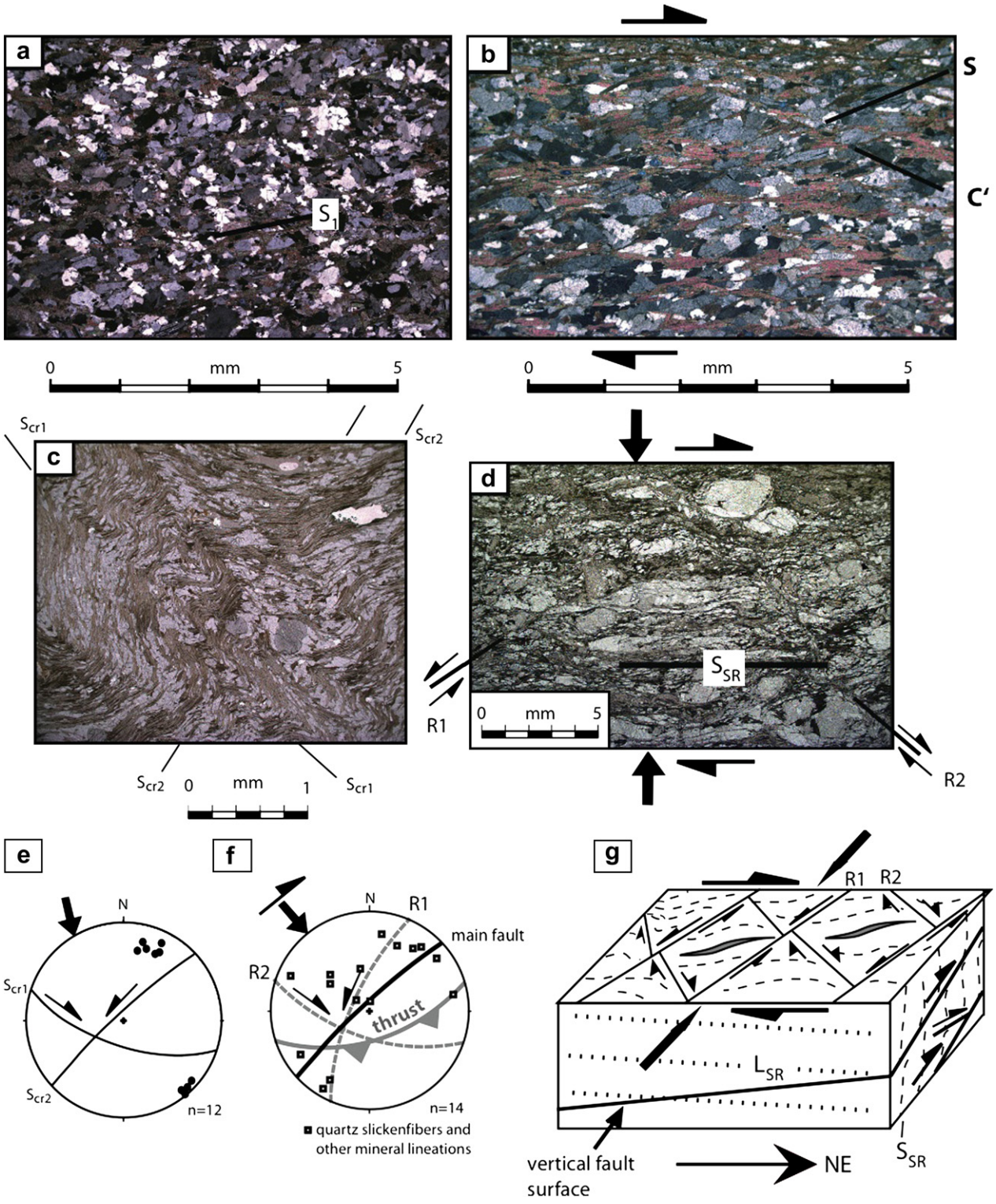

Fig. 8. Evolution of SRSZ structures in thin section. (a) Meta-arenite outside the shear zone at Thompson Sound. (b) C′–S fabric within high strain zone showing an oblique-dextral component of motion. Thin section surface parallels lineation and is perpendicular to foliation. (c) Conjugate crenulation cleavages (S_{cr1}, S_{cr2}) in a low-intermediate strain zone, indicating a component of shortening across the shear zone. This section was cut perpendicular to the S_{cr2} foliation marked in the figure (orientation: 065 80 SE). (d) Conjugate semi-brittle faults indicating a component of shortening across the shear zone at Resolution Island. This section was cut perpendicular to the shear zone foliation marked in the figure (orientation: 047 85 NW). Lower hemisphere, equal area projection showing the two orientations of conjugate crenulation cleavages (e), conjugate faults (f) and mineral lineations, including quartz slickenfibers (f). (g) Block diagram summarizing the relationship among faults.

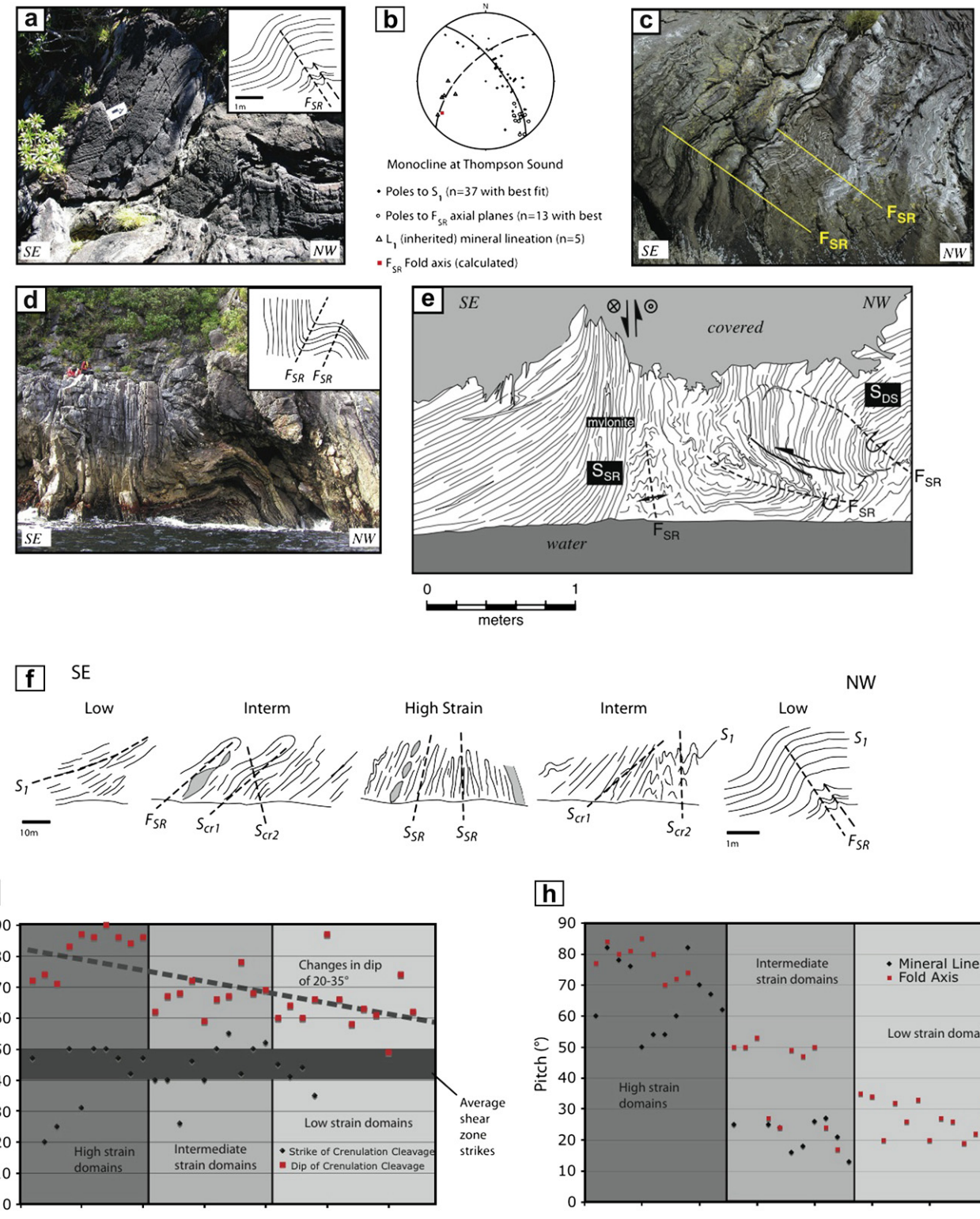

Fig. 9. Structures observed along two NW−SE transects of the SRSZ at Thompson and Doubtful sounds. (a) Photograph of an asymmetric monocline (F_{SR}) in zone of low strain at edge of the shear zone at Thompson Sound. (b) Lower hemisphere, equal area projection showing measurements of F_{SR} axial planes and S_1, and L_1 structures associated with the monocline in (a). (c) Photograph of asymmetric, inclined F_{SR} fold and crenulation cleavage in zone of low-intermediate strain. (d) Photograph of inclined asymmetric folds (F_{SR}) in marble sequence in zone if intermediate strain at Cascada Bay (location in Fig. 3). Inset sketch shows SE-dipping axial plane. (e) Sketch showing vertical profile of oblique-dextral, east-side-down transpressional shear zone. Shear zone deforms older foliation of the Doubtful Sound shear zone (S_{DS}). (f) Summary sketches taken from the profiles shown in Fig. 7 illustrating the criteria that define zones of relative low, intermediate, and high strain that define the SRSZ. (g) Plot showing changes in the strike (black diamonds) and dip (squares) of shear zone cleavage with increasing strain. Note 20−35° change in cleavage dip between low and high strain domains. In contrast the average strike of cleavage in these same areas remains approximately parallel to the shear zone boundaries, with a few exceptions. (h) Plot showing changes in the pitch of mineral lineations (diamonds) and fold axes (squares) with increasing strain. Data are from NE-striking shear zones exposed along Thompson and Doubtful sounds. See text for discussion.

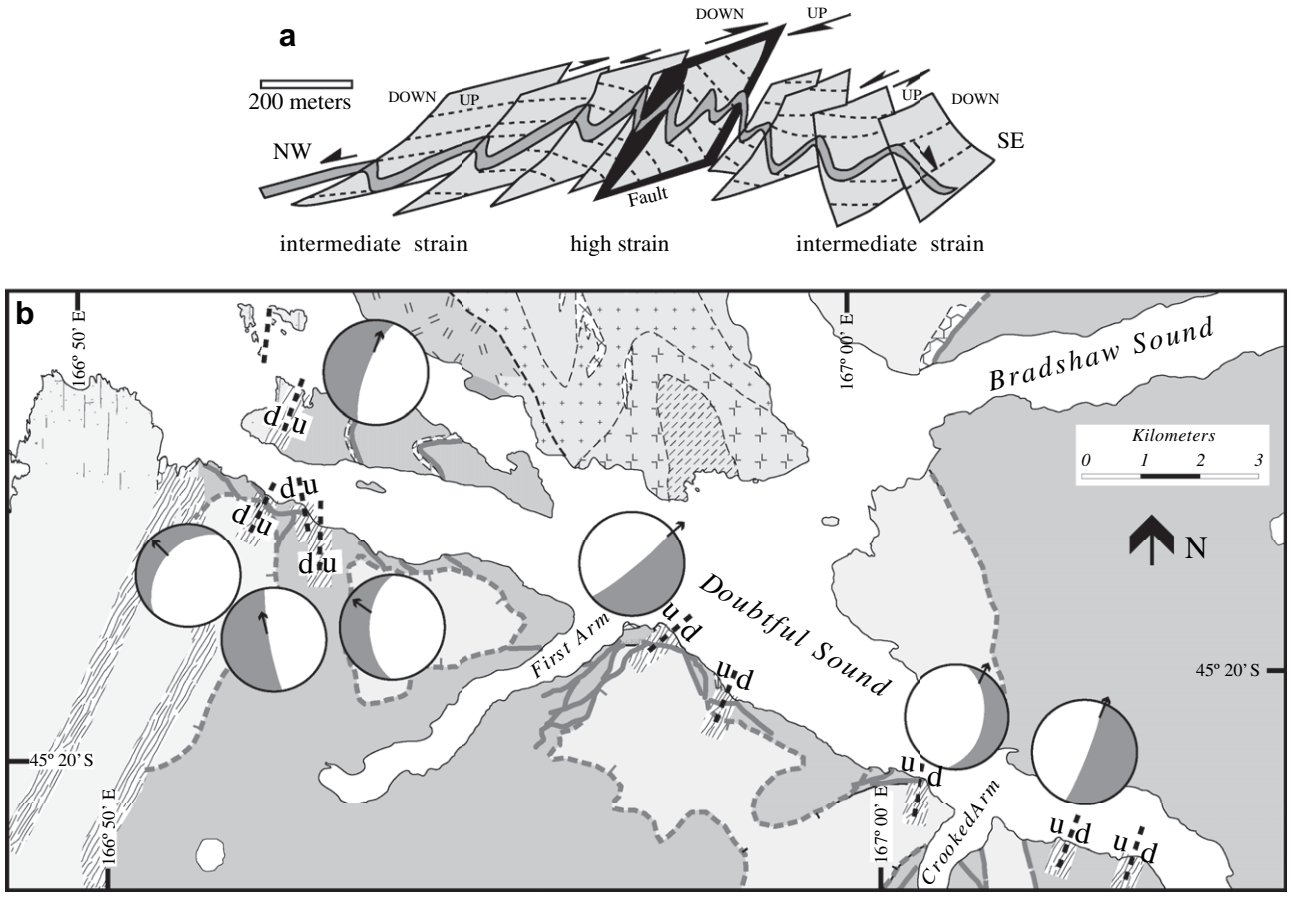

Fig. 10. (a) Perspective diagram showing the steepening of fold axial surfaces and the increase in the pitch of fold axes with increasing strain. Black plane represents a strike-slip fault. Note that intermediate strain zones record evidence of both contractional and strike-slip components of motion. See text for discussion. (b) Map showing the location and kinematics of steep zones of the SRSZ. The hanging wall is shaded grey in each equal area, lower hemisphere projection. The arrow shows the direction of motion of the upper-plate (shaded) relative to the lower-plate as indicated by measured mineral lineations. Great circles are measured orientations of shear zone boundaries. Note that the group to the east of First Arm has an east-side-down component of motion with sinistral slip, and the group to the west has west-side-down component of motion with dextral slip.

kilometers apart. Between these shear zones, the dominant fabric elements are a gently northeast-dipping Doubtful Sound shear zone foliation and a northeast-plunging Doubtful Sound shear zone hornblende lineation. This crosscutting relationship is evidence that the SRSZ is younger and unrelated to the deformation that produced the Doubtful Sound shear zone. The presence of these structures also shows that, whereas we observe SRSZ structures across a wide zone, the deformation is expressed differently in the various lithologies. The more competent dioritic orthogneiss accommodates strain in relatively narrow, widely separated shear zones across several kilometers (Fig. 10), whereas strain is highly localized into a ~250 m-wide zone within the less competent marble sequence at Cascada Bay.

3.3.4. Bauza Island transect

Bauza Island, located ~2 km northeast of Cascada Bay (Fig. 3) displays features that are similar to those at Cascada Bay. Deformation is localized within a ~500 m-thick layer of highly strained and brecciated marble that lies between the Western Fiordland Orthogneiss with Doubtful Sound shear zone foliation and Paleozoic gneiss with pre-existing S_1 foliation (Fig. 7c). The Doubtful Sound shear zone foliation within the orthogneiss varies from dipping shallowly to the northeast to shallowly to the northwest defining broad, open SRSZ folds. We interpret this as a low strain zone showing evidence for the early stages of the SRSZ overprinting the Doubtful Sound shear zone.

As at Cascada Bay, structures related to the SRSZ (F_{SR}, S_{SR}, L_{SR}) are best developed within the marble layer. The pre-existing S_1 foliation in the marble-rich sequence is folded into SRSZ folds. To the east of the area shown in the profile are a series of SRSZ monoclines and recumbent folds with east–southeast-dipping axial planes (e.g. Fig. 7c). High strain zones of SRSZ shear zone foliation overprint the folds. The contact between the marble sequence and the calc-silicate gneiss to the west is highly sheared. Angular fragments of the competent gneiss are suspended within a highly sheared marble matrix.

Farther west, the SRSZ folds in the calc-silicate gneiss gradually becomes open and axial planes dip moderately to the northwest. Measurements of the S_1 foliation around a large

recumbent synform ~500 m west of the marble sequence define an axis that plunges shallowly to the northeast with an interlimb angle of ~38°. The transition from upright, isoclinal folding near the contact (Fig. 7c) to more open folds with axial planes that dip to the NW qualitatively suggest a gradual decrease in strain away from the marble sequence where most of the strain is localized.

3.3.5. Resolution Island transect

On Resolution Island and the north shore of Breaksea Entrance (Fig. 6), the high strain parts of the SRSZ are defined by steep semi-brittle fault zones and a steeply dipping, locally mylonitic greenschist facies foliation that has overprinted all older foliations, including the low-angle extensional Resolution Island shear zone. Quartz forms dynamically recrystallized ribbons and plagioclase displays brittle microfaults and asymmetric pressure shadows of recrystallized quartz and biotite (Fig. 8d). Whereas the dominant foliation is consistently steep within the high strain zones of the SRSZ, biotite and quartz stretching lineations are variably oriented, in part due to the complexity of fault orientations. Nevertheless, two distinctive groups of orientations are recognizable. Quartz–biotite mineral stretching lineations plunge variably to the southwest, west and the northeast. Within mylonite zones of the SRSZ on Resolution Island, hornblende and plagioclase mineral stretching lineations plunge steeply to the northeast and southwest suggesting that, locally, the SRSZ may record amphibolite facies conditions. These two groups of lineations that record different metamorphic grades are indicative of significant exhumation during deformation.

Like the other transects, the geometry of the greenschist facies SRSZ foliation is variable across the shear zone (Fig. 7e). On Resolution Island (Fig. 6), the SRSZ separates the Paleozoic host rock to the west from the Western Fiordland Orthogneiss to the east. Along ~1 km of shoreline the orthogneiss is interlayered with the metasedimentary host rock of probable Paleozoic age. High strain zones are localized within marble and biotite-rich metasedimentary layers. Within these zones, the foliation dips more steeply to the west than outside these zones. To the west of the center of the shear zone the SRSZ foliation dips gently to the west. To the east, a gneissic foliation within the orthogneiss dips variably to the east, northeast and northwest (Fig. 6) and is folded and transposed into the shear zone foliation close to the center of the SRSZ.

Crosscutting the mylonitic zone are networks of brittle and semi-brittle faults that form several distinctive sets. Two of the most prominent sets form near vertical conjugate pairs of minor sinistral and dextral strike-slip faults that strike at high angles to the dominant mylonitic fabric (R1, R2, respectively; Fig. 8d, f, g). Another set of minor thrust faults dips gently to the east and west. Both the conjugate faults and the gently dipping thrusts record contraction at high angles to the shear zone boundaries (Fig. 8f, g). Within and near steep high strain zones, two sets of crenulation cleavage and semi-brittle shear bands overprint the foliation. Here, greenschist facies fault zones deform mylonitic foliation planes into asymmetric lozenges. A well-developed steeply dipping to subvertical set of crenulation cleavage and semi-brittle fault zones also overprints older foliation planes. Adjacent to the fault zones, hornblende-bearing fabrics are retrogressed to chlorite-, epidote- and biotite-bearing assemblages. In these fault zones, biotite and quartz mineral lineations plunge gently to the northeast on shear band foliation planes. Boudinaged amphibolite layers and pegmatites indicate that these directions are true stretching directions.

3.3.6. Kinematics

Changes in the geometry of structures across strain domains (defined in Section 3.3 and Figs. 7 and 9) allowed us to interpret the kinematics of deformation within the SRSZ. Low strain domains generally lack shear zone mineral lineations (L_{SR}) and display asymmetric monoclines. In areas of mica schist, they also are characterized by two crenulation cleavages (S_{cr1}, S_{cr2}). The geometry of these cleavages indicates a component of shortening at high angles to the shear zone boundaries (Fig. 8e). Experimental studies of crenulation cleavage show that conjugate sets form with the axis of maximum principle compression (σ_1) bisecting a ~110° angle between the two cleavage planes (Zheng et al., 2004 and references therein). From this relationship, we infer that σ_1 was oriented northwest–southeast at a high angle to the shear zone boundaries at Thompson Sound (Fig. 8e). In support of this interpretation, the orientation of the conjugate dextral and sinistral faults, as well as thrust faults on Resolution Island, also indicate compression at high angles to the shear zone boundaries (Fig. 8e–g).

In general, sense-of-shear indicators are poorly preserved in low and intermediate strain domains. Where present, they suggest complex three-dimensional displacements. In low strain areas, asymmetric crenulation cleavages and biotite fish show maximum asymmetry on surfaces viewed perpendicular to foliation and perpendicular to fold axes and crenulation lineations. The asymmetries indicate that opposite senses of shear occur across fold axes: a top-down-to-the-southeast sense-of-shear occurs on the east side of antiforms and a top-down-to-the-northwest sense-of-shear on the west side of antiforms. This pattern, and evidence of thickening in the hinges of folds, suggests that flexural flow during NW–SE shortening resulted in folds that evolved into steep high strain zones.

Variations in cleavage orientation and fold geometries provide additional information on the importance of shortening. As finite strain increases across domains, fold axial surfaces (F_{SR}) and the dominant crenulation cleavage (S_{cr2}) rotate from moderately dipping (≥60°) to subvertical (80–90°) (Fig. 9g). In contrast, the strikes of these structures maintain an approximately constant orientation that parallels the steep boundaries of the shear zone. These patterns suggest that shortening was the dominant control on the evolution of shear zone folds and foliations in most places. Nevertheless, in a few intermediate strain zones, fold axes and cleavage strikes are oriented 20–30° from the strike of the shear zone (Fig. 9g), suggesting that the contribution of strike-slip motion also is discernable.

In intermediate strain zones where quartz–biotite mineral lineations are present, shear bands (C′) record the greatest asymmetry on surfaces that parallel the lineation and are perpendicular to foliation. The gentle-moderate plunge (20–30°) of these mineral lineations (L_{SR}, Fig. 9h) and the kinematic indicators show that both reverse and strike-slip components occurred in these domains. For example Fig. 8d shows a C′–S fabric in a meta-arenite from Thompson Sound that records a top-down-to-the-northwest, oblique-dextral sense-of-shear parallel to the mineral lineation. Similar displacements occur at Cascada Bay (Fig. 3). West of this bay, shear senses flip back and forth along the south shore of Doubtful Sound in a manner that is similar to that which occurs on the opposite sides of fold axes in low strain zones at Thompson Sound (Fig. 10b). West of First Arm, shear sense indicators show oblique-dextral shear with a component of west-side-down normal motion (Fig. 10b). East of First Arm, they show oblique-sinistral shear with a component of east-side-down normal motion. These alternating oblique shear senses are consistent with a style of non-coaxial contraction involving NW–SE shortening and a subordinate component of strike-slip deformation. Similar patterns of oblique-slip associated with flexural slip folds have been described in other orogens where they have been interpreted to be related to triclinic transpression (Holdsworth et al., 2002).

Shear sense indicators and changes in the pitch of mineral lineations and fold axes with increasing strain also show that combinations of contraction and strike-slip deformation occur in high strain domains (Fig. 9h). Fold axes display gentle and moderate pitches on axial surfaces in areas of low strain. In intermediate strain domains, quartz–biotite mineral lineations display moderate pitches on cleavage (S_{SR}) planes (Fig. 10a). The pitches of fold axes in these latter domains are variable, reflecting the two sets of crenulation cleavage. One set parallels the mineral lineations, the other is oblique to this lineation. In high strain domains, mineral lineations display moderate (50–60°) to steep (80°) pitches, and fold axes pitch steeply (70–85°). Kinematic indicators in these high strain domains include C′–S fabric, biotite fish, asymmetric deflections of foliation planes, and asymmetric tails on porphyroblasts. In many of these zones the greatest asymmetry occurs on surfaces viewed parallel to the mineral lineation and perpendicular to foliation. However, in some areas it occurs on surfaces viewed oblique to the lineation, indicating that some strike-slip motion occurs across steeply plunging lineations (Fig. 10a). This latter pattern, and the increase in lineation pitch with increasing strain, are expected in zones of triclinic transpression (Robin and Cruden, 1994; Lin et al., 1998) where rapid switches in the direction of finite extension are common (e.g. Tikoff and Greene, 1997; Holdsworth et al., 2002; Marcotte et al., 2005).

On the basis of these observations, we conclude that the SRSZ is a heterogeneous zone of dextral transpression that records contraction at high angles to the shear zone boundaries. Strain is partitioned into a series of spaced, relatively narrow high strain zones that accommodate mostly dextral strike-slip motion with components of flattening and vertical extension. Elsewhere, contraction dominates (non-coaxial contraction, involving mostly shortening with a subordinate component of strike-slip motion) and is accommodated over a much broader region.

4. U/Pb geochronology

To constrain the numerical age of rock fabrics and structures we analyzed zircon with laser-ablation ICPMS. The collector configuration allows simultaneous measurement of ^{204}Pb in a secondary electron multiplier while ^{206}Pb, ^{207}Pb, ^{208}Pb, ^{232}Th, and ^{238}U are measured with Faraday detectors. The samples are from two pegmatite dikes that are deformed by the SRSZ along the southern shore of Doubtful Sound and one felsic dike within the host rock from the western shore of Thompson Sound (sample locations in Fig. 3). All age uncertainties are reported at the 2σ level (analytical methods are in the Supplementary material).

Sample 04-60 is from a pegmatite dike in a narrow zone dominated by S_{SR}. This site lies east of the main zone of continuous deformation associated with the SRSZ in domain III (Fig. 3). The dike cuts the Doubtful Sound shear zone foliation in the Western Fiordland Orthogneiss and displays a steeply dipping SRSZ foliation. These crosscutting relationships indicate that the dike was emplaced after the formation of the Doubtful Sound shear zone foliation and prior to or during the formation of the SRSZ foliation. Thirteen analyses were obtained from zircon grains in sample 04-60. The grains show no sign of inheritance and yielded an age of 88.4 ± 1.2 Ma (Fig. 11a, b). High U/Th ratios (Fig. 11c), with most between 30 and 120, suggest metamorphic zircon growth, although these ratios do not rule out igneous crystallization at the same time (Rubatto et al., 2001; Williams, 2001).

Sample 04-53 is from a pegmatite dike west of the center of the SRSZ along the boundary between domains I and III (Fig. 3). This dike cuts the pre-existing S_1 and S_2 foliations in locally migmatitic Paleozoic metasediment and is faulted. Thirty-eight analyses were conducted on cores and tips of zircon grains. Tips and some young cores define a well-constrained igneous age of 113.4 ± 1.7 Ma (Fig. 11d, e). Most cores show older inherited ages. Robust peaks defined by multiple analyses are shown on the age probability plot (Fig. 11g) at 335 Ma, 555 Ma, and 767 Ma. Additional age peaks are present, but defined by only one analysis. Most U/Th values are typical of igneous zircon grown (U/Th < 10), but some tips have extreme U/Th values (Fig. 11f), suggesting that some metamorphic zircon growth accompanied or followed the igneous crystallization of most of the zircon. We interpret the igneous age to reflect zircon crystallization during partial melting in the migmatite and/or contact metamorphism during the intrusion of Early Cretaceous plutons associated with the Western Fiordland Orthogneiss.

Sample 05-135 is from a felsic (quartz + plagioclase) dike within the metasedimentary host rock. The sample location is within domain I near the boundary with domain II from the western shore of Thompson Sound (Fig. 3). The dike cuts

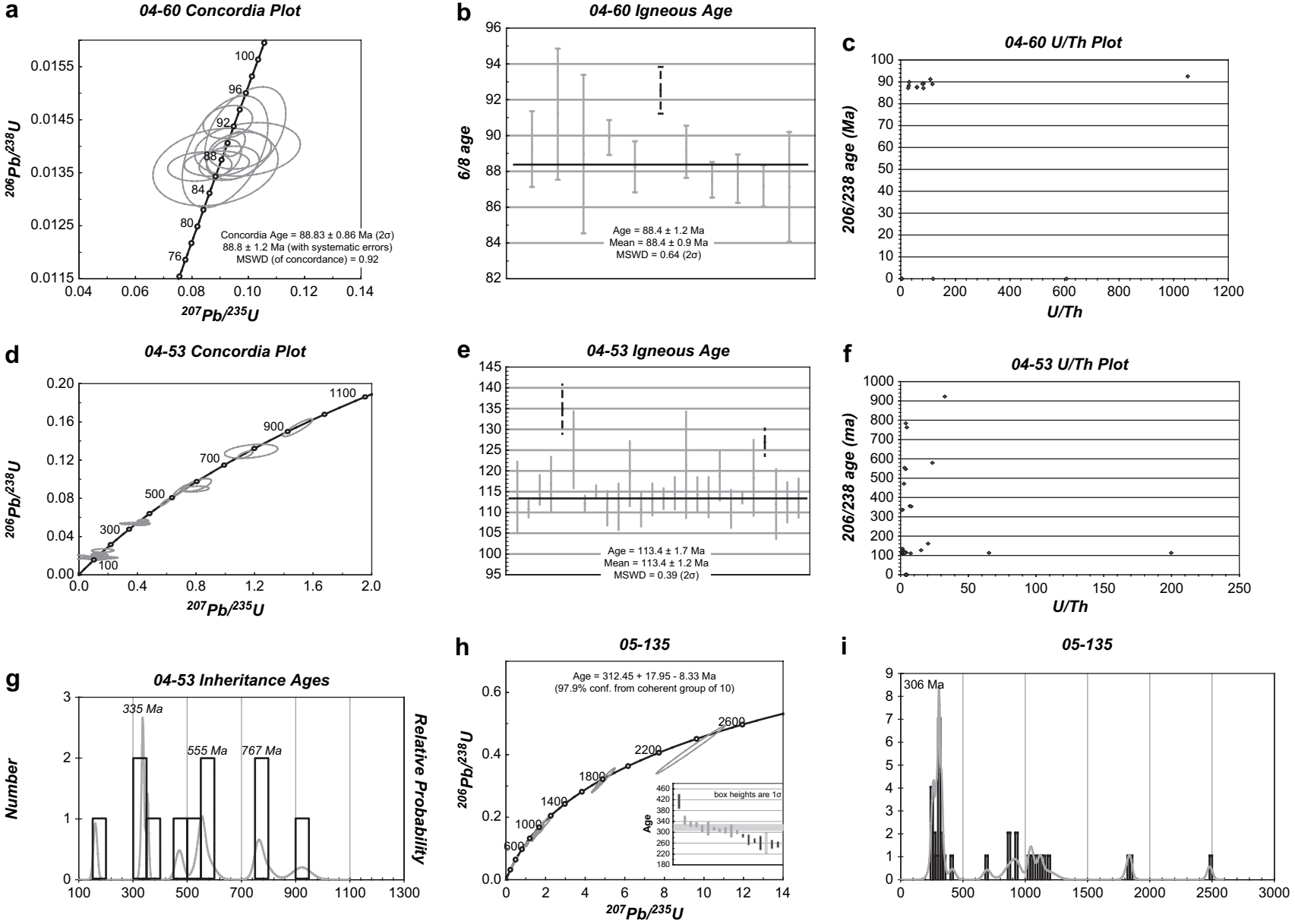

Fig. 11. U/Pb isotopic data collected from zircon using laser-ablation ICPMS. Plots (a), (d) and (h) are concordia plots that show all analyses from samples 04–60, 04–53, and 05–135, respectively. See Fig. 3 for sample locations. Error ellipses on these plots are presented at 68.3% confidence. Plots (b) and (e) show the distribution of $^{206}Pb/^{238}U$ ages measured for samples 04–60 and 04–53. Inset in plot (h) shows an age distribution plot for a coherent group of ten anlayses from sample 04–53. The ages are shown with two uncertainties. Those labeled "age" include all errors, while the "mean" includes only the random (measurement) errors. The age with a larger uncertainty is reported in the text. Note that the uncertainties are reported at the 2σ level while the error bars for each analysis are shown at the 1σ level. Plots (c) and (f) show U/Th versus $^{206}Pb/^{238}U$ ages. See text for a description of how these plots help us discriminate between igneous and metamorphic zircon. Plot (g) is an age probability plot of core analyses from sample 04–53. Plot (i) is an age distribution plot of all analyses.

the dominant flat foliation (S_1 and S_2) but is also tightly folded within the F_2 folds that deform S_1 and S_2. From this field relationship, we interpret the dike to have formed after the S_1 foliation and before F_2 folds. Thirty-two analyses were conducted on zircon grains, 27 from cores of grains and five from tips or rims. The age distribution plot (Fig. 11i) shows that there is significant spread in the ages. Cores of zircon grains record age peaks of Proterozoic and Paleozoic age with the strongest peak at ~306 Ma. A group of 10 coherent analyses define an approximate age of $312.45 + 17.95, -8.33$ Ma (Fig. 11h).

5. Discussion

5.1. Interpretation of U/Pb geochronology

The analyses of zircon from sample 05-135 (Fig. 11h, i) show that the S_1 and S_2 foliations of domain I records several tectono-thermal events. The zircon is complex due to the effects of both Pb loss and inheritance, and record a range of Proterozoic and Paleozoic ages. The youngest recorded event is Carboniferous with an average of $312.45 + 17.95/-8.33$ Ma and a peak at 306 Ma according to the zircon density distribution (Fig. 11i). These ages are slightly younger than those obtained by Ireland and Gibson (1998) and Gibson and Ireland (1999) who showed that high-*P* metamorphism occurred at ~330 Ma following a period (340–370 Ma) of arc magmatism. The lack of zircon overgrowth or the crystallization of Mesozoic and younger zircon shows that this section of the crust remained relatively cool and undisturbed by fluids since ~306 Ma. The results also show that the dominant foliation in domain I records only minor effects of Cretaceous extension and magmatism (*cf.* Klepeis et al., 2007).

The results of zircon analyses from sample 04-60 (Fig. 11a–c) allow us to constrain the duration of extension in Fiordland. The ages and crosscutting relationships of the dike that yielded this sample indicate that extension ceased by 88.4 ± 1.2 Ma. This age is younger than other published zircon $^{206}Pb/^{238}U$ ages from the Western Fiordland Orthogneiss and represents the first determination of when extension in Fiordland ended using U/Pb techniques. Ion probe analyses of zircon from the Western Fiordland Orthogneiss by Gibson et al. (1988) yielded $^{206}Pb/^{238}U$ ages of 119 ± 5 Ma (1σ) in an amphibolite facies mylonite, and 126 ± 3 Ma (1σ) in a granulite facies orthogneiss. SHRIMP analysis of zircon by Hollis et al. (2004) yielded $^{206}Pb/^{238}U$ ages of 115.6 ± 2.4 Ma (2σ) in a metadioritic sample of the orthogneiss, and 114 ± 2.2 Ma (2σ) in a sample of sheared garnet granulite in the orthogneiss. U/Pb analyses of zircon from a syntectonic dike obtained by Klepeis et al. (2007) indicated that deformation in the Doubtful Sound shear zone began before and outlasted 102.1 ± 1.8 Ma. Our result that extension ended by ~88 Ma is compatible with these published ages. It also indicates that the SRSZ formed after 88.4 ± 1.2 Ma.

The results of zircon analyses from sample 04-53 allowed us to evaluate the relative proximity of rocks located west of the SRSZ to Early Cretaceous plutons. The 113.4 ± 1.7 Ma igneous age from this sample (Fig. 11g) represents one of the youngest ages associated with Early Cretaceous arc magmatism and contact metamorphism in Fiordland. Similar crystallization ages from the Western Fiordland Orthogneiss in the range 116–113 Ma have been obtained from elsewhere the granulite belt (Gibson et al., 1988; Tulloch and Kimbrough, 2003; Hollis et al., 2004). Hollis et al. (2004) obtained SHRIMP analyses of zircon grains from calc-silicate paragneiss above the orthogneiss at Crooked Arm, which yielded a strong peak in $^{206}Pb/^{238}U$ ages at 117.7 ± 2.8 Ma (2σ) and lesser peaks at *c.* 600–500 Ma and 1100–900 Ma. Zircon from Crooked Arm yielded a pronounced peak at 116 ± 2 Ma (2σ) with Paleozoic inheritance, most notably a peak at ~480 Ma (Ireland and Gibson, 1998). These age relationships and the occurrence of migmatite suggest that this rock experienced igneous crystallization, contact metamorphism, and dike emplacement. These observations place it in close proximity to either the Western Fiordland Orthogneiss or the Breaksea Gneiss during the final stages of the emplacement of their protoliths.

The results from samples 04-53 and 05-135 (Fig. 11b–i) also allow us to evaluate the possible terrane affiliations of rocks on either side of the SRSZ. The broad similarity of the protolith lithology and the pattern of inherited zircon ages from these samples (especially the young Carboniferous ages) with other published ages from metasedimentary rock at Doubtful Sound (Ireland and Gibson, 1998; Gibson and Ireland, 1999) supports the interpretation that the Paleozoic metasediments located west and east of the SRSZ are part of the same, or similar, Paleozoic terrane. Confirmation of this interpretation awaits additional analyses on both sides of the shear zone.

The interpretations that sample 04-53 was in close proximity to Early Cretaceous plutons and that Paleozoic host rock on both sides of the SRSZ are similar implies that deformation in the SRSZ involved strike-slip displacements of only a few kilometers. One hypothesis is that the migmatite at site 04-53 originated from an area where the westernmost strand of the SRSZ has cut across and displaced the contact aureole of the Breaksea Gneiss a few kilometers south of Dagg Sound (Fig. 7a). Alternatively, oblique top-down-to-the-northwest displacement on the SRSZ at the Cascada Bay could have dropped migmatitic host rock down from above the Western Fiordland Orthogneiss along Doubtful Sound. Both possibilities are consistent with our finding that deformation in the SRSZ was dominated by contraction at high angles to its boundaries and involved less than 20 km of strike-slip displacement and only a few kilometers of vertical motion. Nevertheless, the exact magnitude of displacement along the SRSZ is unknown and awaits detailed mapping and the dating of units between Breaksea and Dagg sounds.

5.2. Interpretation of transpressional shear zone evolution

Any kinematic model of the SRSZ must explain the following observations: (1) contraction at high angles to the shear

zone boundaries; (2) fold axial surfaces and cleavage planes that strike parallel to the shear zone at all stages of development, but progressively steepen to subvertical with increasing strain (Fig. 9g, h); (3) The flipping of shear sense from oblique-sinistral (east-side-down component) to oblique-dextral (west-side-down component) across zones of intermediate and high strain (e.g. Fig. 10a, b); and (4) The occurrence of high strain zones where mineral lineations and fold axes pitch steeply and kinematic indicators record strike-slip motion in narrow zones. Below we present a kinematic model (Fig. 12) of triclinic transpression where zones of mostly strike-slip deformation are narrow and contraction is accommodated heterogeneously over a relatively large region. The model also illustrates how the folding of pre-existing foliations and the steepening of axial surfaces during shortening resulted in steep, spaced zones of high strain during transpression.

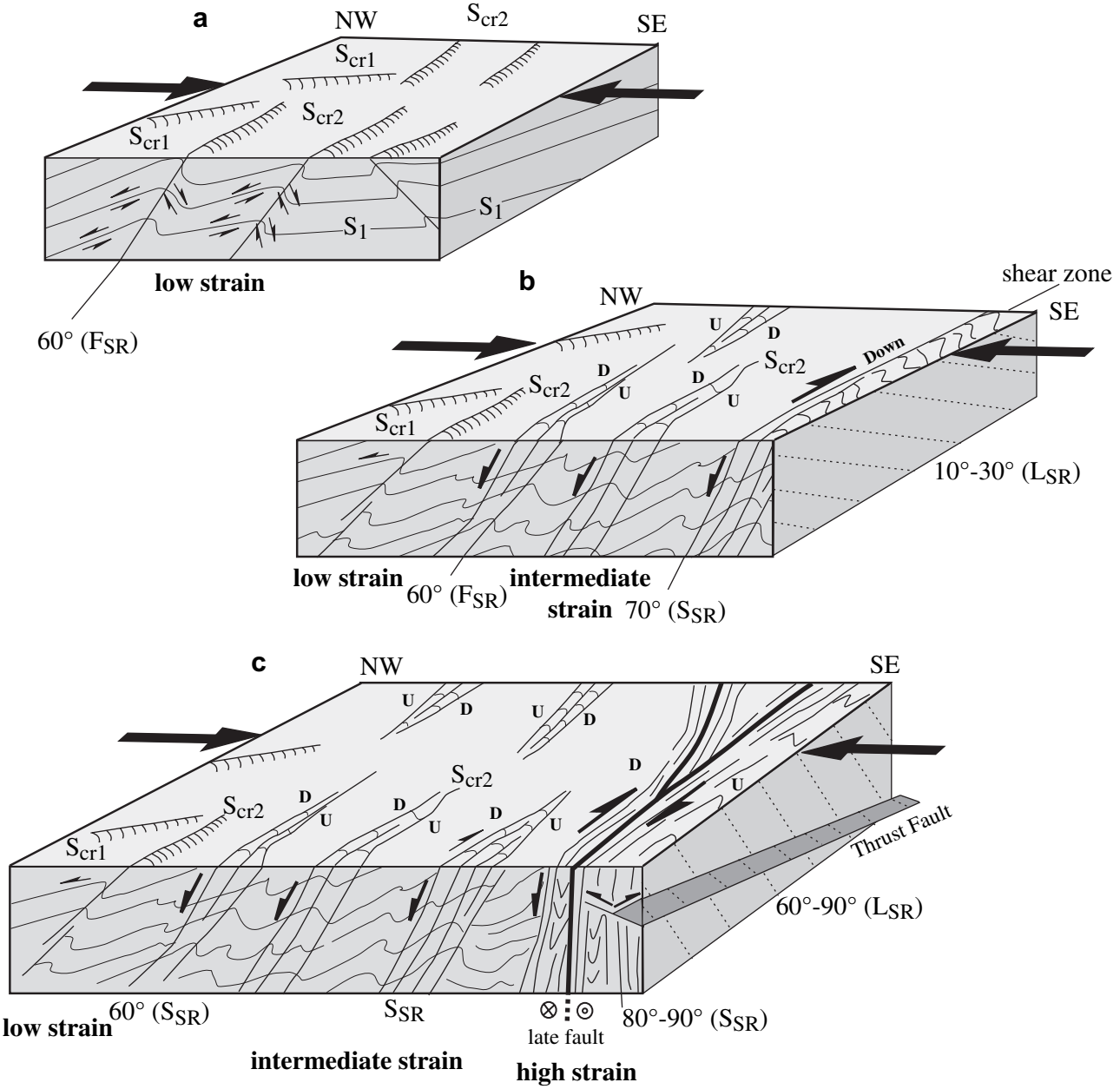

Fig. 12. Block diagrams showing the progressive evolution of structures in the SRSZ. (a) Layer parallel shortening forms monoclines and box folds. Conjugate crenulation cleavages record shortening at high angles to shear zone boundaries. Shear sense varies on either side of the fold hinges as a result of flexural slip. (b) Continued deformation results in the progressive tightening and steepening of folds. Cleavage intensifies in the steepened limbs of tight-isoclinal folds, forming zones of high strain. Shear sense varies on either side of the fold hinges as a result of flexural flow. Combined shearing and shortening creates a shear zone cleavage that accommodates oblique-slip. (c) As strain accumulates, cleavage rotates to subvertical and mineral lineations and fold axes plunge steeply. Combined dextral shearing and shortening occur in these zones of high strain. At a regional scale, shortening with a subordinate component of strike-slip deformation is distributed over a large region. In contrast, zones of mostly strike-slip deformation are localized into relatively narrow zones. The formation of late conjugate strike-slip faults and minor thrusts in high strain zones also reflect this localization of strain.

Deformation is inferred to have begun with the formation of asymmetric monoclines and open folds of pre-existing regional foliations (S_1/S_2, S_{DS}) (Fig. 12a). The axial planes of the monoclines and crenulation cleavages (S_{cr1}, S_{cr2}) dip moderately (60°) to the northwest and southeast (e.g. Figs. 7c and 9a). With continued shortening, the monoclines tightened into asymmetric folds (F_{SR}) and their axial planes rotated to subvertical (Fig. 12b). Conjugate crenulation cleavages and minor thrusts developed that record shortening at high angles to the shear zone boundaries. Slip or ductile shear between rock layers during folding resulted in shear senses that change from oblique-west-side-down to oblique-east-side-down across the hinges of the folds. This type of kinematic pattern commonly results where folds form by flexural slip or flexural flow between layers in a rock, and is well-documented in zones where a pre-existing mechanical anisotropy controls folding (Holdsworth et al., 2002; Coke et al., 2003).

Continued shortening resulted in the rotation of F_{SR} fold axial planes to near vertical as strain increased (Fig. 12c). A penetrative axial planar foliation (S_{SR}) developed from the flattening and the intensification of the steeper of the two crenulation cleavages. These zones of S_{SR} foliations and tight-isoclinal folds define steep zones of high strain. Pre-existing fabrics are transposed into the SRSZ foliation. High strain zones accommodated both shortening and components of strike-slip motion and near vertical extrusion. Conjugate brittle faults (R1, R2) and minor thrusts formed and record shortening and oblique-slip in narrow, branching fault zones.

This style of strain partitioning invites a comparison to other zones of partitioned transpression. At Marble Cove in Newfoundland, Goodwin and Williams (1996) reported a broad domain in a transpressive shear zone where stretching lineations plunge steeply and accommodate mostly reverse motion with a component of dextral shear. Narrow zones of high strain display shallowly plunging lineations and accommodated mostly dextral shear with a component of reverse motion. This style, where shortening is accommodated over a broader region than the strike-slip component, is similar to that which we observed in the SRSZ. However, the geometry of lineations and distribution of sense-of-shear indicators we observed are different than those in the Marble Cove example. We observed the steepest lineations in narrow zones of high strain. More shallowly plunging lineations occur heterogeneously in zones of intermediate strain. This pattern may partly reflect the poor preservation of mineral lineations outside of high strain domains. However, it also appears to reflect a situation where strike-slip deformation is partitioned into narrow zones in *both* intermediate and high strain domains. A similar pattern, where areas dominated by contraction develop punctuated strain heterogeneities that reflect some strike-slip motion, has been described by van Noorden et al. (2007). These authors attribute the pattern to the incipient stages of strain partitioning where organized domains of contraction and strike-slip motion have not yet formed. Our observations, where this pattern occurs in some intermediate strain areas, are consistent with this interpretation.

In our model, vertical lineations reflect triclinic bulk strain where components of shortening and vertical extension control the orientation of structures at the margins of high strain domains (e.g. Tikoff and Greene, 1997; Holdsworth et al., 2002; Marcotte et al., 2005). In the centers of these domains steep faults and narrow zones of ductile strain accommodate the strike-slip component. Some strike-slip motion is evidence by shear indicators that occur across the steep lineation away from the faults. Similar high strain zones where triclinic transpression is partitioned into zones of non-coaxial contraction (contraction at high angles to the shear zone boundaries with components of dip-slip simple shear and strike-slip simple shear) have been described by Holdsworth et al. (2002). Our observations are compatible with this study and suggest a heterogeneous partitioning of transpressional deformation into broad zones of non-coaxial shortening (shortening plus subordinate components of vertical extension and strike-slip motion) and narrow zones of strike-slip-dominated deformation.

The Fiordland example also illustrates how lithologic variability and competency contrasts influenced the evolution of a zone of transpression. Fig. 7a shows that the SRSZ closely follows the contacts between the Western Fiordland Orthogneiss/Breaksea Gneiss and Paleozoic host rock, where rheological contrasts are most pronounced. Within Paleozoic host rock, where compositional layers of different competency that define the inherited Paleozoic foliation are thin (<1 m), the shear zone folds are short-wavelength and tight. In contrast, where metadioritic rocks of the Western Fiordland Orthogneiss and Doubtful Sound shear zone consist of thick layers of gneiss and mylonite (>10 m), long-wavelength, open folds accommodate layer-perpendicular shortening.

5.3. Regional significance of transpression

The small amount of isotopic data that constrain the absolute age of transpression in Fiordland allow for only tentative correlation with other structures. Our U/Pb zircon analyses indicate that the SRSZ is younger than 88.4 ± 1.2 Ma. U/Pb analyses of rutile from Crooked Arm (Fig. 3) have yielded ages from 73.0 ± 0.5 Ma to 65.8 ± 0.5 Ma, suggesting that temperatures in this section of the crust cooled to below ~400–450 °C by these times (Flowers et al., 2005). Since mineral assemblages within the SRSZ record metamorphism mostly at the greenschist facies and lower, these rutile ages could represent a lower limit for the age of the SRSZ. However, transpression is inconsistent with the documented regional tectonic setting at this time, which was dominated by extension and the opening of the Tasman Sea (Gaina et al., 1998; Kula et al., 2005).

The style of deformation in the SRSZ invites comparison with both the Anita shear zone (Fig. 1) and to offshore strands of the Alpine fault. In the latter, Klepeis et al. (1999) identified a phase of contraction-dominated dextral transpression (their D_3 event) that is similar to what we have documented in some parts of the SRSZ. Both shear zones show domains that are dominated by folding, subhorizontal shortening, and a subvertical foliation. However, although it postdates Late

Cretaceous extension, the numerical age of the transpressional fabric in the Anita shear zone also is unknown.

The SRSZ occurs inboard of and parallels active traces of the Australian–Pacific plate boundary located offshore (Frohlich et al., 1997; Barnes et al., 2001, 2005; Cande and Stock, 2004). In central Fiordland, the Alpine fault is ~10–30 km from the shoreline and is composed of many branching fault segments (Barnes et al., 2001, 2005). Several major strike-slip faults of the Resolution Ridge segment occur along the strike of the SRSZ to the south (Sutherland, 1999; Barnes et al., 2001; Lebrun et al., 2003; Barnes and Nicol, 2004). This alignment and similarities between the SRSZ and transpressional strands of the Alpine fault suggests that the former has played a role in accommodating some of the obliquely convergent motion between the Australian and Pacific Plates. This also seems plausible given that the SRSZ displays faults that are kinematically similar to late Tertiary faults exposed near Milford Sound (Sutherland and Norris, 1995; Norris and Cooper, 2001; Claypool et al., 2002). We therefore suggest that at least the most recent phase of deformation in the SRSZ is related to the late Tertiary dextral motion along the Alpine fault. If correct, our results suggest that a significant, albeit unquantified, component of margin-perpendicular shortening is accommodated inside Fiordland by networks of steep transpressional zones. Regardless of whether this is correct, the SRSZ is the largest transpressional shear zone yet discovered inside Fiordland.

6. Conclusions

A 10 km-wide zone of transpression, the SRSZ, affects at least 800 km^2 of continental crust inboard of the southernmost segment of the Alpine fault in Fiordland, New Zealand. Regionally, the SRSZ traces the boundary between Early Cretaceous granulite facies orthogneiss and Paleozoic metasedimentary rock. The SRSZ is composed of steep, narrow zones of relatively high strain. The geometry of folds, conjugate faults, secondary thrusts, and conjugate crenulation cleavages in the shear zone record contraction at high angles to its boundaries. The dominant process by which the steep zones of high strain formed involved the development of moderately inclined, asymmetric folds that were progressively tightened and rotated to vertical as strains accumulated. The folding of pre-existing layering resulted in a kinematic pattern characterized by shear senses that alternate from oblique-sinistral (east-side-down component) to oblique-dextral (west-side-down component) across high strain zones. These steep zones accommodated both dip-slip and strike-slip components of motion at scales of 10–100 m. The shear zone records a style of partitioned triclinic transpression where strike-slip motion localized into relatively narrow zones while non-coaxial contraction (flattening plus a subordinate component of strike-slip motion) was accommodated over a large region. It also illustrates how pre-existing structural and lithologic heterogeneities are important factors in controlling the evolution of subvertical structures commonly viewed as diagnostic of transpression.

At its northern end, the SRSZ formed in Paleozoic rock where a regional pre-existing fabric formed during a period of contraction and magmatism of mostly Carboniferous (~312–306 Ma) age. Along its central and southern segments, the shear zone cuts across Early Cretaceous plutons and gently dipping extensional shear zones. New U/Pb zircon analyses indicate that Cretaceous magmatism had ended by 113.4 ± 1.7 Ma and extension had ceased by 88.4 ± 1.2 Ma. Zircon analyses show similarities in protolith age and igneous and metamorphic histories across the shear zone, indicating that it is not a major terrane boundary associated with the large-scale (>20 km) dispersal of rock units along the margin.

The age and style of transpression in the shear zone invite comparisons with offshore segments of the Alpine fault system. Within the limits of available ages, the similarities among these structures suggest that transpression could have occurred during the late Tertiary, indicating that a significant amount of shortening at high angles to the Alpine fault may be accommodated within Fiordland.

Acknowledgements

This work resulted in a MSc thesis by DSK. Funding was provided by the National Science Foundation (EAR-0087323, EAR-0337111 to KAK and EAR-0443387 to GG); Geological Society of America funding to DSK; and an AAPG Grant-in-Aid to DSK. We thank Mo Turnbull and R. Jongens for providing detailed maps and data from the interior of Secretary Island (Fig. 3). A. Tulloch and N. Mortimer provided helpful assistance. A. Schoonmaker provided comments on the manuscript. We are grateful to Laurel Goodwin and Mike Williams for thoughtful reviews. We thank the Department of Conservation in Te Anau for permission to visit and sample localities in Fiordland. M. De Paoli, G. 'Rusty' Rigg, and D. Karn helped with field work.

Appendix A. Supplementary data

Supplementary data associated with this article can be found, in the online version, at doi: 10.1016/j.jsg.2007.12.004.

References

Allibone, A.H., Tulloch, A.J., 1997. Metasedimentary, granitoid and gabbroic rocks from central Stewart Island, New Zealand. New Zealand Journal of Geology and Geophysics 40, 53–68.

Allibone, A.H., Turnbull, I., Milan, L., Carroll, S., Daczko, N., 2005. The granulite facies Western Fiordland Orthogneiss in Southwest Fiordland, paper presented at 50th Annual Meeting, Geological Society of New Zealand, Kaikoura, New Zealand, 28 November–1 December.

Barnes, P.M., Nicol, A., 2004. Formation of an active thrust triangle zone associated with structural inversion in a subduction setting, eastern New Zealand. Tectonics 23 (1). Art. No. TC1015.

Barnes, P.M., Sutherland, R., Davy, B., Delteil, J., 2001. Rapid creation and destruction of sedimentary basins on mature strike-slip faults: an example

from the offshore Alpine fault, New Zealand. Journal of Structural Geology 23, 1727–1739.

Barnes, P.M., Sutherland, R., Delteil, J., 2005. Strike-slip structure and sedimentary basins of the southern Alpine fault, Fiordland, New Zealand. GSA Bulletin 117 (3/4), 411–435.

Berryman, K.R., Beanland, S., Cooper, A.F., Cutten, H.N., Norris, R.J., Wood, P.R., 1992. The Alpine fault, New Zealand: variation in Quaternary structural style and geomorphic expression. Annales Tectonicae 6, 126–163.

Bhattacharyya, P., Hudleston, P., 2001. Strain in ductile shear zones in the Caledonides of northern Sweden: a three-dimensional puzzle. Journal of Structural Geology 23, 1549–1565.

Bradshaw, J.Y., 1989. Early Cretaceous vein-related garnet granulite in Fiordland, southwest New Zealand: a case for infiltration of mantle-derived CO_2-rich fluids. Journal of Geology 97, 697–717.

Bradshaw, J.Y., 1990. Geology of crystalline rocks of northern Fiordland; details of the granulite facies western Fiordland Orthogneiss and associated rock units. New Zealand Journal of Geology and Geophysics 33, 465–484.

Butler, R.W.H., Spencer, S., Griffiths, H.M., 1998. The structural response to evolving plate kinematics during transpression: evolution of the Lebanese restraining bend of the Dead Sea Transform. In: Holdsworth, R.E., Strachan, R.A., Dewey, J.F. (Eds.), Continental Transpressional and Transtensional Tectonics. Geological Society of London Special Publications, vol. 135, pp. 81–106.

Cande, S.C., Stock, J.M., 2004. Pacific-Antarctic-Australia motion and the formation of the Macquarie Plate. Geophysical Journal International 157 (1), 399–414.

Clarke, G.L., Klepeis, K.A., Daczko, N.R., 2000. Cretaceous high-P granulites at Milford Sound, New Zealand: metamorphic history and emplacement in a convergent margin setting. Journal of Metamorphic Geology 14, 441–452.

Claypool, A., Klepeis, K., Dockrill, B., Clarke, G., Zwingmann, H., 2002. Structure and kinematics of oblique continental convergence in Northern Fiordland, New Zealand. Tectonophysics 359 (3–4), 329–358.

Coke, C., Dias, R., Ribeiro, A., 2003. Rheologically induced structural anomalies in transpressive regimes. Journal of Structural Geology 25 (3), 409–420.

Czeck, D.M., Hudleston, P.J., 2003. Testing models for obliquely plunging lineations in transpression: a natural example and theoretical discussion. Journal of Structural Geology 25, 959–982.

Daczko, N.R., Klepeis, K.A., Clarke, G.L., 2001. Evidence of early Cretaceous collisional-style orogenesis in northern Fiordland, New Zealand and its effects on the evolution of the lower crust. Journal of Structural Geology 23, 693–713.

Flowers, R.M., Bowring, S.A., Tulloch, A.J., Klepeis, K.A., 2005. Burial and exhumation of a magmatic arc, Fiordland, New Zealand. Geology 33 (1), 17–20.

Fossen, H., Tikoff, B., 1993. The deformation matrix for simultaneous simple shearing, pure shearing and volume change, and its application to transpression–transtension tectonics. Journal of Structural Geology 15, 413–422.

Frohlich, C., Coffin, M.F., Massell, C., Mann, P., Schuur, C.L., Davis, S.D., Jones, T., Karner, G., 1997. Constraints on Macquarie Ridge tectonics provided by Harvard focal mechanisms and teleseismic earthquake locations. Journal of Geophysical Research 102 (B3), 5029–5041.

Fuis, G.S., et al., 2003. Fault systems of the 1971 San Fernando and 1994 Northridge earthquakes, southern California: relocated aftershocks and seismic images from LARSE II. Geology 31, 171–174.

Gaina, C., Muller, D.R., Royer, J.Y., Stock, J., Hardebeck, J., Symonds, P., 1998. The tectonic history of the Tasman Sea: a puzzle with 13 pieces. Journal of Geophysical Research 103 (B6), 12413–12433.

Gibson, G.M., 1990. Uplift & exhumation of middle & lower crustal rocks in an extensional tectonic setting, Fiordland, New Zealand. In: Fountain, D.M., Salisbury, M.H. (Eds.), Exposed Cross-sections of the Continental Crust. NATO ASI Series, Series C: Mathematical and Physical Sciences, vol. 317. Kluwer Academic Publishers, Netherlands, pp. 71–101.

Gibson, G.M., Ireland, T.R., 1995. Granulite formation during continental extension in Fiordland, New Zealand. Nature 375, 479–482.

Gibson, G.M., Ireland, T.R., 1999. Black Giants Anorthosite, New Zealand: a Paleozoic analogue of Archean stratiform anorthosites and implications for the formation of Archean high-grade gneiss terranes. Geology 27 (2), 131–134.

Gibson, G.M., McDougall, I., Ireland, T.R., 1988. Age constraints on metamorphism and the development of a metamorphic core complex in Fiordland, southern New Zealand. Geology 16, 405–408.

Goodwin, L.B., Williams, P.F., 1996. Deformation path partitioning within a transpressive shear zone, Marble Cove, Newfoundland. Journal of Structural Geology 18 (8), 975–990.

Harland, W.B., 1971. Tectonic transpression in Caledonian Spitsbergen. Geological Magazine 108, 27–42.

Hill, E.J., 1995. A deep crustal shear zone exposed in western Fiordland, New Zealand. Tectonics 14, 1172–1181.

Holdsworth, R.E., Tavarnelli, E., Clegg, P., Pinheiro, R.V.L., Jones, R.R., McCaffrey, K.J.W., 2002. Domainal deformation patterns and strain partitioning during transpression: an example from the Southern Uplands terrane, Scotland. Journal of the Geological Society, London 159, 401–415.

Hollis, J.A., Clarke, G.L., Klepeis, K.A., Daczko, N.R., Ireland, T.R., 2004. The regional significance of Cretaceous magmatism and metamorphism in Fiordland, New Zealand, from U/Pb zircon geochronology. Journal of Metamorphic Geology 22, 607–627.

House, M.A., Gurnis, M., Kamp, P.J.J., Sutherland, R., 2002. Uplift in the Fiordland region, New Zealand: implications for incipient subduction. Science 297 (5589), 2038–2041.

Ireland, T.R., Gibson, G.M., 1998. SHRIMP monazite and zircon geochronology of high-grade metamorphism in New Zealand. Journal of Metamorphic Geology 16, 149–167.

Jiang, D., Lin, S., Williams, P.F., 2001. Deformation path in high-strain zones, with reference to slip partitioning in transpressional plate-boundary regions. Journal of Structural Geology 23, 991–1005.

Jones, R.R., Holdsworth, R.E., Bailey, W., 1997. Lateral extrusion in transpression zones: the importance of boundary conditions. Journal of Structural Geology 19, 1201–1217.

Jones, R.R., Holdsworth, R.E., Clegg, P., McCaffrey, K., Tavarnelli, E., 2004. Inclined transpression. Journal of Structural Geology 26, 1531–1548.

Klepeis, K.A., Clarke, G.L., Gehrels, G., Vervoort, J., 2004. Processes controlling vertical coupling and decoupling between the upper and lower crust of orogens: results from Fiordland, New Zealand. Journal of Structural Geology 26, 765–791.

Klepeis, K.A., Daczko, N.R., Clarke, G.L., 1999. Kinematic vorticity and tectonic significance of superposed mylonites in a major lower crustal shear zone, northern Fiordland, New Zealand. Journal of Structural Geology 21, 1385–1405.

Klepeis, K.A., King, D.S., De Paoli, M., Clarke, G.L., Gehrels, G., 2007. Interaction of strong lower and weak middle crust during lithospheric extension in western New Zealand. Tectonics 26, TC4017.

Kula, J.L., Tulloch, A.J., Spell, T.L., Wells, M.L., 2005. Timing of continental extension leading to separation of eastern New Zealand from West Antarctica; $^{40}Ar/^{39}Ar$ thermochronometry from Stewart Island, NZ. Geological Society of America Abstracts with Programs 37 (7), 3.

Lamarche, G., Collot, J.-Y., Wood, R.A., Sosson, M., Sutherland, R., Delteil, J., 1997. The Oligocene-Miocene Pacific–Australia plate boundary, south of New Zealand: evolution from oceanic spreading to strike-slip faulting. Earth and Planetary Science Letters 148, 129–139.

Lamarche, G., Lebrun, J.F., 2000. Transition from strike-slip faulting to oblique subduction: active tectonics at the Puysegur Margin, South New Zealand. Tectonophysics 316, 67–89.

Lebrun, J.F., Lamarche, G., Collot, J.Y., 2003. Subduction initiation at a strike-slip plate boundary: the Cenozoic Pacific–Australian plate boundary, south of New Zealand. Journal of Geophysical Research 108 (B9). Art. No. 2453.

Lin, S., Jiang, D., Williams, P.F., 1998. Transpression (or transtension) zones of triclinic symmetry natural example and theoretical modelling. Geological Society of London Special Publications, vol. 135, pp. 41–57.

Little, T.A., 1996. Faulting-related displacement gradients and strain adjacent to the Awatere strike-slip fault in New Zealand. Journal of Structural Geology 18, 321–340.

Marcotte, S.B., Klepeis, K.A., Clarke, G.L., Gehrels, G., Hollis, J.A., 2005. Intra-arc transpression in the lower crust and its relationship to magmatism in a Mesozoic magmatic arc. Tectonophysics 407, 135–163.

Markley, M., Norris, R.J., 1999. Structure and neotectonics of the Blackstone Hill Antiform, Central Otago, New Zealand. New Zealand Journal of Geology and Geophysics 42, 205–218.

Mattinson, J.L., Kimbrough, D.L., Bradshaw, J.Y., 1986. Western Fiordland Orthogneiss: early Cretaceous arc magmatism and granulite facies metamorphism, New Zealand. Contributions to Mineralogy and Petrology 92, 383–392.

McCaffrey, R., 1992. Oblique plate convergence, slip vectors, and forearc deformation. Journal of Geophysical Research 97, 8905–8915.

McCulloch, M.T., Bradshaw, J.Y., Taylor, S.R., 1987. Sm–Nd and Rb–Sr isotopic and geochemical systematics in Phanerozoic granulites from Fiordland, southwest New Zealand. Contributions to Mineralogy and Petrology 97, 183–195.

Milan, L.A., Daczko, N.R., Turnbull, I., Allibone, A.H., 2005. Thermobarometry of an Early Cretaceous high-pressure contact metamorphic aureole near Resolution Island, Fiordland, New Zealand. Geological Society of Australia Abstracts 76, 79–85.

Mortimer, N., Gans, P.B., Calvert, A., Walker, N., 1999. Geology and thermochronometry of the east edge of the Median Batholith (Median Tectonic Zone); a new perspective on Permian to Cretaceous crustal growth of New Zealand. The Island Arc 8, 404–425.

Mount, V.S., Suppe, J., 1987. State of stress near the San Andreas fault: implications for wrench tectonics. Geology 15, 1143–1146.

van Noorden, M., Sintubin, M., Darboux, J.R., 2007. Incipient strain partitioning in a slate belt: evidence from the early Variscan Monts d'Arree slate belt (Brittany, France). Journal of Structural Geology 29 (5), 837–849.

Norris, R.J., Cooper, A.F., 1995. Origin of small-scale segmentation and transpressional thrusting along the Alpine fault, New Zealand. GSA Bulletin 107 (2), 231–240.

Norris, R.J., Cooper, A.F., 2001. Late Quaternary slip rates and slip partitioning on the Alpine fault, New Zealand. Journal of Structural Geology 23, 507–520.

Norris, R.J., Koons, P.O., Cooper, A.F., 1990. The obliquely convergent plate boundary in the South Island of New Zealand: implications for ancient collision zones. Journal of Structural Geology 12, 715–725.

Oliver, G.J.H., 1990. An exposed cross-section of continental crust, Doubtful Sound, Fiordland, New Zealand; geophysical and geological setting. In: Salisbury, M.H., Fountain, D.M. (Eds.), Exposed Cross-sections of the Continental Crust. Kluwer Academic Publishers, Netherlands, pp. 43–69.

Oliver, G.J.H., 1977. Feldspathic hornblende and garnet granulites and associated anorthosite pegmatites from Doubtful Sound, Fiordland, New Zealand. Contributions to Mineralogy and Petrology 65, 111–121.

Oliver, G.J.H., 1980. Geology of the granulite and amphibolite facies gneisses of doubtful sound, Fiordland, New Zealand. New Zealand Journal of Geology and Geophysics 23 (1), 27–41.

Oliver, G.J.H., Coggon, J.H., 1979. Crustal structure of Fiordland, New Zealand. Tectonophysics 54, 253–292.

Robin, P.-Y.F., Cruden, A.R., 1994. Strain and vorticity patterns in ideally ductile transpression zones. Journal of Structural Geology 16 (4), 447–466.

Rubatto, D., Williams, I.S., Buck, I.S., 2001. Zircon and monazite response to prograde metamorphism in the Reynolds Range, central Australia. Contributions to Mineralogy and Petrology 140, 458–468.

Sanderson, D.J., Marchini, W.R.D., 1984. Transpression. Journal of Structural Geology 6, 449–457.

Spell, T.L., McDougall, I., Tulloch, A.J., 2000. Thermochronologic constraints on the breakup of the Pacific Gondwana margin: the Paparoa metamorphic core complex, South Island, New Zealand. Tectonics 19 (3), 433–451.

Sutherland, R., 1999. Basement geology and tectonic development of the greater New Zealand region: an interpretation from regional magnetic data. Tectonophysics 308, 341–362.

Sutherland, R., Berryman, K., Norris, R., 2006. Quaternary slip rate and geomorphology of the Alpine fault: implications for kinematics and seismic hazard in southwest New Zealand. Bulletin of the Geological Society America 118, 464–474, doi:10.1130/B25627.1.

Sutherland, R., Davey, F., Beavan, J., 2000. Plate boundary deformation in South Island, New Zealand is related to inherited lithospheric structure. Earth and Planetary Science Letters 177, 141–151.

Sutherland, R., Norris, R.J., 1995. Late Quaternary displacement rate, paleoseismicity, and geomorphic evolution of the Alpine fault: evidence from Hokuri Creek, South Westland, New Zealand. New Zealand Journal of Geology and Geophysics 38, 419–430.

Tavarnelli, E., Holdsworth, R.E., Clegg, P., Jones, R.R., McCaffrey, K.J.W., 2004. The anatomy and evolution of a transpressional imbricate zone, Southern Uplands, Scotland. Journal of Structural Geology 26 (8), 1341–1360.

Teyssier, C., Tikoff, B., Markley, M., 1995. Oblique plate motion and continental tectonics. Geology 23, 447–450.

Tikoff, B., Greene, D., 1997. Stretching lineations in transpressional shear zones: an example from the Sierra Nevada Batholith, California. Journal of Structural Geology 19 (1), 29–39.

Tikoff, B., Teyssier, C., Water, C., 2002. Clutch tectonics and the partial attachment of lithospheric layers. European Geophysical Society Special Publication 1, 57–73.

Tulloch, A.J., Kimbrough, D.L., 1989. The Paparoa metamorphic core complex, New Zealand: cretaceous extension associated with fragmentation of the Pacific margin of Gondwana. Tectonics 8, 1217–1234.

Tulloch, A.J., Kimbrough, D.L., 2003. Paired plutonic belts in convergent margins and the development of high Sr/Y magmatism: the Peninsular Ranges Batholith of California and the Median Batholith of New Zealand. In: Johnson, S.E., Paterson, S.R., Fletcher, J.M., Girth, G.H., Kimbrough, D.L., Martin-Barajas, A. (Eds.), Tectonic Evolution of Northwestern Mexico and the Southwestern USA. Geological Society of America Special Paper, vol. 374, pp. 275–295.

Turnbull, I.M., Allibone, AH., Jongens, R., Fraser, HL., and Tulloch, AJ., 2005. Progress on QMAP Fiordland, Paper Presented at 50th Annual Meeting, Geological Society of New Zealand, Kaikoura, New Zealand, 28 November–1 December.

Turnbull, I.M., Allibone, A.H., 2003. Geology of the Murihiku Area. Institute of Geological and Nuclear Sciences 1:250,000 geological map 20. 1 sheet and 74p. Institute of Geological and Nuclear Sciences Limited, Lower Hutt, New Zealand.

Vauchez, A., Tommasi, A., Barruol, G., 1998. Rheological heterogeneity, mechanical anisotropy and deformation of the continental lithosphere. Tectonophysics 296, 61–86.

Wellman, H.W., 1953. Data for the study of recent and late Pleistocene faulting in the South Island of New Zealand. New Zealand Journal of Science and Technology B34, 270–288.

Williams, I.S., 2001. Response of detrital zircon and monazite, and their U/Pb isotopic systems, to regional metamorphism and host-rock partial melting, Cooma Complex, southeastern Australia. Australian Journal of Earth Sciences 48, 557–580.

Wood, B.L., 1960. Sheet 27, Fiordland. Geological Map of New Zealand. New Zealand Geological Survey, Department of Scientific and Industrial Research. scale 1:250,000.

Zheng, Y., Wang, T., Ma, M., Davis, G.A., 2004. Maximum effective moment criterion and the origin of low-angle normal faults. Journal of Structural Geology 26, 271–285.